博士論文（要約）

Development of regenerative medicine for subacute spinal cord injury in dogs using intravenous administration of bone marrow-derived mesenchymal stem cells.

(骨髄由来間葉系幹細胞の静脈投与による犬の亜急性期脊髄損傷に対する脊髄再生医療の開発)

武田　妙

1. Spinal cord injury in dogs

Spinal cord injury (SCI) caused by intervertebral disk disease (IVDD) or trauma is common neurological disorder in dogs (Aikawa *et al.*, 2012). SCI causes mild to severe back pain and various neurological deficits including paresis or paralysis depending on the severity of the damage. Pharmacological treatment using analgesia and anti-inflammatory agents is adapted to ambulatory patients, while surgical treatment is a main stay for patients with non-ambulatory paresis and plegia. However, the prognosis of dogs with severe SCI is usually poor. In case of thoracholumber IVDD which is the most common cause of SCI in dogs, the prognosis after surgical treatment for dogs with deep pain perception is generally satisfactory and most of the dogs regain the ability to walk. In contrast, dogs without deep pain perception show worse outcome with an irreversible motor and sensory disabilities even after surgery (Aikawa *et al.*, 2012; Rabinowitz *et al.*, 2008) and an overall recovery rate of voluntary walking ability is approximately estimated to 50% (Jeffery *et al.*, 2016). One of the reasons of this poor outcome is that surgical treatment cannot repair the injured spinal cord itself but only remove the mechanical force on the spinal cord. Therefore, to overcome the insufficient , A., Bain severe SCI patients, a novel approach to repair the injured spinal cord tissue should be explored.

2. Regenerative therapy for SCI using stem cells in human and veterinary medicine

It had been believed that damaged central nervous system (CNS) does not regenerate, however recent studies have shown that CNS involves various stem cells which contribute to intrinsic support to tissue homeostasis. Though application of stem cells for SCI is expected as a promising treatment in human and veterinary medicine, various types of stem cells have been proposed as cell sources for regenerative therapy for SCI such as induced neural stem cells and embryonic stem cells (ESCs), pluripotent stem cells (iPSCs) and mesenchymal stem cells (MSCs).

iPSCs were established by introducing *Oct4, Sox2, Klf4* and *c-myc* genes into somatic cells such as skin fibroblasts or blood cells to reprogram into pluripotent stem cells like ESCs (Takahashi *et al.*, 2006). Pluripotency and genetic phenotypes of iPSCs are almost comparable to ESCs, however, iPSCs have the advantage for clinical application because the ethical problem using embryos is not concerned. Thus, for this decade, iPSCs have taken place of ESCs as cell source of regenerative therapy for various diseases. Particularly for human SCI and other neurological diseases, the most possible therapeutic strategy using iPSCs has been considered to transplant neural precursor/stem cells induced from iPSCs to replace the injured neurons and

oligodendrocytes (Nakamura *et al.*, 2013). However, the induction of reprograming genes includes another issue, a risk of tumorigenesis. Therefore, researchers have been enthusiastic to improve reprograming methods to generate safer iPS cells with lower risk of tumorigenesis (Yoshihara *et al.*, 2017). As a result, the first clinical trial of transplantation of neural stem/progenitor cells derived from human iPS cells for SCI patients has been approved by Ministry of Health of Japan in 2019 (https://www.keio.ac.jp/ja/press-releases/2018/11/28/28-49692/). Nevertheless, considerably careful monitoring should be required in the clinical trial. Unfortunately, there has been no report demonstrated generation of canine iPSCs available for clinical settings. So far, several researchers have demonstrated that canine iPSCs are induced with the similar reprograming method as human iPSCs, however, the pluripotency is not completely elucidated, and the risk of tumorigenesis remains to be solved (Betts *et al.*, 2015; Cebrian-Serrano *et al.*, 2013).

MSCs are another promising cell source for regenerative therapy for SCI and defined as multipotent progenitor cells with the capacity of self-renewal and differentiation into mesenchymal lineage including adipocytes, osteoblasts, and chondrocytes (Dominici *et al.*, 2006). MSCs reside in stroma of various organs such as bone marrow and adipose tissue, and maintain the tissue homeostasis through

replacement of the damaged cells and producing various growth factors and chemokines (Valtieri *et al.*, 2008). Therapeutic strategy of regenerative therapy using MSCs can be established based on the concept to apply this essential role of MSCs in the body to repair injured tissue.

MSCs are easily isolated from adult tissues with no ethical concerns and minimal cost, and the possibility of tumorigenesis is extremely low as compared with iPSCs. Therefore, MSCs is highly available cell source especially in veterinary medicine and MSCs-based therapy has already applied to some canine SCI patients (Penha *et al.*, 2014). Even though several reports showed the successful outcomes obtained when MSCs were transplanted into dogs with SCI, it is likely that the present regenerative therapy using MSCs are performed without scientific evidences to guarantee its efficacy and safety. Most of clinical trials for canine SCI patients only demonstrated the outcome in functional recovery and failed to discuss the mechanism of therapeutic effects precisely. The US Food and Drug Administration also criticized the prevalence of MSCs-based therapy blind to adequate evidence of efficacy and safety in US veterinary clinics (Cyranoski *et al.*, 2013). To resolve this problem, it should be required to determine whether the canine MSCs used for regenerative therapy have potential to

contribute to tissue repair and reasonable therapeutic strategy should be established based on the scientific evidences.

3. **Desirable properties of MSCs required as an useful cell source for regenerative therapy of SCI**.

3.1. Homing ability

Homing ability indicates a capacity of migrating into the sites of injury and inflammation. MSCs naturally possess this ability to contribute to maintain tissue homeostasis, and it have been well-documented that bone marrow MSCs travel to injured skin and contribute to skin closure by incorporating into skin structure (Badiavas *et al.*, 2003; Fathke *et al.*, 2004). Thus, homing ability allow to apply systemic administration of MSCs which is less invasive to treat various diseases including SCI (Hu *et al.*, 2013; Ra *et al.*, 2011). Especially for SCI, direct and local transplantation to the injured spinal cord requires invasive surgical procedures for patients. Therefore, systemic administration is a desirable approach to transplant MSCs to the injured spinal cord, and MSCs for this purpose should be qualified to have homing ability prior to application.

It is suggested that CXC chemokine receptors and ligands play important roles in homing of MSCs into the injured spinal cord. Among these factors, several reports suggest that the mechanism by which MSCs migrate to the injury site mainly depends on chemoattractant activity between CXC chemokine receptor 4 (CXCR4) and its chemo-attractants CXC chemokine ligand 12 (CXCL12) (Hocking, 2014). CXCR4 is known to be expressed in murine and human MSCs (Gong *et al.,* 2014; Sordi *et al.*, 2009; Wynn *et al.*, 2004), and its expression in canine MSCs is also expected. Additionally, CXCL12 is known to upregulate at injured site especially in subacute phase of SCI (Bai *et al.*, 2016; Tysseling *et al.*, 2011). Thus, it is hypothesiezed that MSCs systemically administrated into subacute SCI home into the injured site via CXCR4-CXCL12 axis.

3.2. Trophic effects

Another prerequisite of MSCs to treat SCI is trophic effects through secreting humoral molecules including growth factors such as neurotrophic and angiogenic factors to contribute to tissue repair of SCI (Chamberlain, *et al.*, 2007; Iyer *et al.*, 2017; Urdzikova *et al.*, 2014). Neurotrophic factors such as nerve growth factor (NGF) and brain derived neural factor (BDNF) is reported to be secreted from MSCs and can

improve functional recovery through protecting neurons from apoptosis and prolonging motor neurons (Crigler *et al.*, 2006; Kim *et al.*, 2010; Wilkins *et al.*, 2009). Angiogenesis after SCI also plays an important role in tissue repair and regeneration through resupply of oxygen and nutrition to the lesion sites. Several kinds of angiogenic factors including vascular endothelial growth factors (VEGF), hepatocyte growth factors (HGF), connective tissue growth factors (CTGF) and fibroblast growth factor -2 (FGF-2) are reported to be released from transplanted MSCs to injured tissue and contribute to neovascularization (Beckermann *et al.*, 2008; Li *et al.*, 2016; Oskowitz *et al.*, 2011; Tögel *et al.*, 2005; Wang *et al.*, 2006; Wu *et al.*, 2007).

3.3 Transdifferentiation into neuronal cells

MSCs are defined to have multi-differentiation ability to mesenchymal lineage including adipocytes, osteoblasts, and chondrocytes. However, the transdifferentiation potential of MSCs into other types of cells such as neurons and oligodendrocytes has also been described in vitro and in vivo (Nakano *et al.*, 2013; Dasari *et al.*, 2007). Therefore, it has been believed that transdifferention of MSCs into neural lineage contributes to replace damaged cells after SCI. However, so far, transdifferentiaion into neural lineage have been mainly addressed based on the expression level of specific

markers for neural cells and evidence of functional integration to damaged spinal cord have not been shown (Ryu *et al.*, 2012). Therefore, the contribution of MSC transdifferentiation into neural cells is thought to be relatively minor when compared to trophic effects (Wu *et al.*, 2007; Rustad *et al.*, 2012)

4. Pathology of spinal cord injury

To achieve successful outcome in regenerative therapy for SCI, to exactly understand the pathology of SCI is important. The pathology of acute phase of SCI is consisted of inflammatory responses such as upregulation of inflammatory cytokines, excitatory neurotransmitters and free radicals (Nakamura *et al.*, 2013). The inflammatory milieu in this phase is not suitable for engraftment of MSCs and to exert their ability. On the contrary, in the chronic phase, the main pathology changes to glial scar formation which prevents axonal regeneration. Considering these pathological features of SCI, subacute phase seems to be an optimal target period for regenerative therapy due to less inflammation milieu and glial scar formation (Fawcett *et al.*, 1999; Ide *et al.*, 2010; Jing *et al.*, 2017).

5. Origin of MSCs

MSCs can be isolated from various tissues such as bone marrow, adipose tissue, periosteum, synovium, and deciduous teeth (Kikuta *et al.*, 2013), however, the characteristics and the potentials have been reported to differ depending on the cell origin and the isolation method (Kisiel *et al.*, 2012; de Bakker *et al.*, 2013). Therefore, it is required to examine whether the MSCs used actually possess the expected potential.

Among MSCs derived from various tissues, bone marrow MSCs (BMMSCs) and adipose tissue-derived MSCs (ADMSCs) are the richest sources of MSCs in dogs and have the advantages of being easily and relatively noninvasibely obtained compared with other tissues (Fortier *et al.*, 2011). Therefore, canine BMMSCs and ADMSCs have been well characterized and already been applied for various disease including SCI in dogs (Lin *et al.*, 2017). However, a few disadvantages in regarding to clinical use these cells for clinics have been also reported. A disadvantage of BMMSCs is lower proliferative ability, and there is the time lag of 3 to 6 weeks from bone marrow aspirate until treatment (Fortier *et al.*, 2011). Contrary to BMMACs, ADMSCs have high proliferative ability, however, ADMSCs represent a heterogenous cell population contaminated by endothelial cells, smooth muscle cells, pericytes and blood cells such as monocytes and lymphocytes (Matsumoto *et al.*, 2008; Yoshimura *et al.*, 2006). The

heterogenous property of ADMSCs makes it difficult to understand the therapeutic effects obtained by ADMSCs.

A novel canine MSCs called as bone marrow peri-adipocyte cells (BM-PACs) have been recently established. BM-PACs is isolated from cells adhering to adipocytes in bone marrow using a ceiling culture method (Lin *et al.*, 2017). BM-PACs have a greater proliferative ability and a higher multi-differentiation ability comparing to conventional canine BMMSCs isolated by adhering culture of mononuclear cells in bone marrow. Therefore, BM-PACs are regarded as superior MSCs comparing to BMMSCs, and the prominent proliferative ability of BM-PACs allows to harvest adequate number of cells for clinical use approximately in 1 week. Thus, the use of BM-PACs expands the opportunity for dogs with SCI to receive the cell therapy in subacute phase. Further, it would be possible to apply autologous cells to the cell therapy. Since autologous MSCs generally have higher therapeutic effects than heterogenous MSCs without any immunological concerns, (Jung *et al.*, 2009) BM-PACs can be a promising cell source for regenerative therapy for dogs with subacute SCI.

6. Purpose of the study

The purpose of this study was to establish an evidence-based regenerative therapy for canine subacute SCI. From the pathological findings of SCI and therapeutic property of MSCs mentioned above, it was hypothesized that BM-PACs systemically administrated in subacute phase of SCI may home to the injured spinal cord depending on their CXCR4 expression level and increase of CXCL12 expression at the injury site, and induce functional recovery through their growth factor secretion. Therefore, by investigating the homing ability and therapeutic potential of BM-PACs, this study may able to suggest an novel and effective regenerative strategy for canine SCI. And moreover, assessing the safety of intravenous administration of autologous BM-PACs may broad the availability of stem cell therapy for SCI dogs. To clarify the properties and therapeutic effects of BM-PACs, DFs were subjected as counterparts of BM-PACs and the properties of BM-PACs were compared with those of DFs to delineate the differences between MSCs and non-MSCs.

In Chapter 1, homing ability of BM-PACs was evaluated based on CXCR4 expression and chemotaxis assay towards CXCL12. In Chapter 2, gene expression levels of neural and angiogenic factors of BM-PACs and DFs were compared, and secretion ability of those with significant difference of gene expression were detected were further analyzed with ELISA. Angiogenic ability was also examined using culture supernatant

of BM-PACs and human umbilical vein endothelial cell (HUVEC). In Chapter 3, Intravenous administration of BM-PACs to a subacute SCI nude model mice were performed, and homing to the injured site was evaluated using in vivo imaging system (IVIS). Therapeutic effects of BM-PACs and DFs through their homing ability and trophic effects were examined by comparison of functional recovery and histological analysis *in vivo*. Lastly in Chapter 4, the safety of IV administration of BM-PACs and whether homing ability of BM-PACs in healthy dog were able to confirm using super paramagnetic iron oxide (SPIO) nanoparticle which is reported as an alternative tool for *in vivo* cell tracking using MRI (Sykova *et al.*, 2007) were evaluated.

Chapter 1

Investigation of chemotaxis ability of BM-PACs through CXCR4-CXCL12 axis

Introduction

Homing ability of cells which responds to injury or inflammation is a key characteristic to develop a regenerative therapy for SCI by intravenous administration of MSCs. Although the effectiveness of intravenous administration of canine MSCs for SCI has been demonstrated by several researchers (Kim *et al.*, 2015; Penha *et al.*, 2014), no study has clarified the homing ability of canine MSCs.

It has been reported that chemokines produced at the injury site and the receptors to these chemokines expressed on MSCs play important roles in homing in human and murine (Honczarenko *et al.*, 2006). CXC-chemokine ligand 12 (CXCL12) is a member of the CXC chemokine family which binds to its highly specific corresponding receptor CXC-chemokine receptor 4 (CXCR4). CXCL12 and CXCR4 are well-known factors by which human and murine MSCs home to the injured tissue (Hocking, 2015; Gong *et al.*, 2014; Sordi *et al.*, 2009; Wynn *et al.*, 2004). It is reported that CXCL12 was upregulated in subacute phase of SCI (Anwar *et al.*, 2016). Therefore, investigation of the expression of CXCR4 in BM-PACs and the chemoattractant property toward CXCL12 is essential to assess homing ability of BM-PACs into the injured spinal cord in subacute phase of SCI.

In chapter 1, to investigate the chemotaxis ability of BM-PACs through CXCR4-CXCL12 axis, I examined CXCR4 expression and chemotaxis toward CXCL12

of BM-PACs was evaluated. Here, to clearly define the property of BM-PACs as MSCs, comparative approach using skin dermal fibroblast (DFs) as non-stem mesenchymal cells was applied. CXCR4 expression and chemotaxis property of BM-PACs was compared with those of DFs.

Materials and Methods

Animals

All animal experiments were approved by the Animal Care Committee of Graduate School of Agricultural and Life Sciences, the University of Tokyo (Approval No.P17-106).

Culture of BM-PACs and DFs

Seven healthy young beagles (3 males and 4 females, 2-3 years-old, weighing an average of 10.2 kg) were anesthetized with propofol (Maruishi pharm., Osaka, Japan) and 2.0% isoflurane (Fujifilm Wako, Osaka, Japan) in oxygen. Bone marrow was harvested from humer using a sterilized 15-gauge bone marrow biopsy needle (Angiotech Pharmaceuticals, Inc., Vancouver, Canada). Then, 1×1 cm of full-thickness skin was aseptically excised from the dorsal part of thorax using a surgical knife. Dogs were given single injection of 2 mg/kg robenacoxib (Onsior, Elanco Japan K.K., Tokyo, Japan) and 5 mg/kg of enrofloxacin (Baytril, Bayer HealthCare, Tokyo, Japan) subcutaneously to control post operative pain and prevent infection.

Canine BM-PACs were isolated and cultured according to the previous studies (Lin et al, 2017). Briefly, bone marrow was subjected to density gradient centrifugation

using Ficoal-Paque Plus solution (GE Healthcare, Little Chalfont, United Kingdom). After centrifugation, the top adipose layer was collected and washed with Dulbecco's modified Eagle's medium (DMEM) (Invitrogen, Carlsbad, CA) containing 10% FBS (Lot no.1168943, Invitrogen) and 1% penicillin-streptomycin/amphotericin-B (Wako). After washed 2-3 times, the adipose layer was placed in 25-cm^2 flask (Sumitomo Bakelite Co., Inc., Japan) completely filled with DMEM supplemented with 20% FBS and 1% antibiotics. Then, ceiling culture was maintained at 37℃ in a humidified 5% CO_2 incubator for 7 days. If the cells did not reach 80% confluency within 7 days, the flask was inverted and the culture was maintained with changing culture medium every 3 days. The cells reached over 80% confluency were detached with 0.25% trypsin/1 mM ethylene diamine tetra acetic acid (EDTA) solution (Wako) and cryopreserved until use.

Canine DFs were cultured according to a previous study (Khammanit et al, 2008) with a minor modification. After washed three times in phosphate buffered saline (PBS) containing 1% antibiotics and trimmed fat tissue, the skin graft was placed on a 90-mm culture dish (Sumitomo Bakelite Co., Inc., Japan) with the dermal side facing downward. Culture was maintained with DMEM supplemented with 10% FBS and 1% antibiotics at 37℃ in 5% CO_2 and 95% humidity with changing medium every 3 days.

Cells were detached using EDTA solution at 80% confluency and cryopreserved until use.

Immunocytochemistry

BM-PACs and DFs were seeded at a density of 8×10^3 cells in each well of a 8-well chamber slide (Thermo Fisher Scientific, Whalthman, MA) and kept at 37℃ in 5% CO2. After incubated for 24 hr, cells were washed and fixed with 4% paraformaldehyde (PFA) for 15 min. Fixed cells were washed with PBS three times for 5 min each and permeabilized by tris-buffered saline-containing 0.3% tween 20 (TBS-T) for 15 min. Permeabilized cells were blocked by TBS-T containing 10% normal goat serum (NGS) and incubating for 1 hr at room temperature. After blocking, rabbit monoclonal anti-CXCR4 antibody (1:200, ab124824, Abcam Cambridge, United Kingdom) were applied and incubated over night at 4℃. After washed three times for 5 min each with TBS-T, Alexa Flour 568 conjugated-goat anti-rabbit IgG (1:400, ab175695, Abcam) was applied at room temperature for 1 hr, and the nuclei were counterstained with DAPI (1:1000, Promocell, Heidelberg, Germany).

Chemotaxis assay

Chemotaxis assay was carried out in trans-wells with 8-μm pore polycarbonate membrane insert and 24-well plate (Corning Costar, Cambridge, MA). BM-PACs and DFs at a density of 2 ×10^5 cells per well in 0.1 ml of DMEM contained 1% FBS were placed in the upper insert chamber of the trans-well assembly. The lower chamber contained 0.5 ml of DMEM with 1% FBS and human recombinant SDF-1α/CXCL12 (R&D Systems, McKinley Place, NM) at a different concentration (0, 10, 50 and 100 ng/ml). After incubation at 37℃ and 5% CO2 for 24 hr, the upper surface of the membrane was gently scraped by a cotton swab to remove non-migrating cells and washed with distilled water three times. The membrane was then fixed in 70% ethanol for 10 min and stained in 0.2% crystal violet for 3 min. The number of migrating cells was determined by counting in 5 random fields per well under the microscope at a magnification of ×40. Experiments were independently performed three times.

Statistical analysis

All data were expressed as mean ± standard division (SD). Comparisons were made by using One-way ANOVA with post hoc analysis followed by Dunnett's test for multiple group comparison to detect statistical significance. Comparisons between 2 groups were evaluated with the Student's t-test. Statistical analyses were performed

using EZR software package (Saitama Medical Center/Jichi Medical University, Saitama, Japan). Statistical significance of mean value of samples were accepted at $p < 0.05$.

Results

Expression of chemokine receptor CXCR4 in BM-PACs and DFs

Immunocytochemistry revealed that BM-PACs and DFs show similar apparently positive expression of CXCR4 in cytoplasm and nucleus (Fig. 1).

Chemotactic ability of BM-PACs and DFs toward CXCL12

DFs and BM-PACs showed chemotactic response to CXCL12 in a concentration dependent manner. DFs showed significant increase in number of migrate cells only at 100 ng/ml of CXCL12, while BM-PACs showed significant increase in number of migration at lower concentration (50, 100 ng/ml) (Fig. 2). These chemotactic responses of DFs and BM-PACs were completely blocked by adding CXCR4 antagonist, AMD3100 (Fig. 3).

Discussion

In this chapter, homing ability of BM-PACs to the injured spinal cord in subacute phase of SCI was estimated *in vitro* by CXCR4 expression and chemoattractant property toward CXCL12 by comparing with those of DFs.

Immunocytochemistry revealed that BM-PACs and DFs showed apparently positive expression of CXCR4 mainly in cytoplasm. It is reported that human and murine MSCs also express CXCR4 dominantly in the cytoplasm, and internalized CXCR4 receptor is mobilized to the cell surface and coupled with its ligand CXCL12 to activate chemoattractant function. Even though the expression level of CXCR4 receptors at the cell surface is low, human and murine MSCs successfully showed chemotaxis toward CXCL12 (Hocking, 2015; Wynn *et al.*, 2004). Therefore, it seems reasonable to suppose that BM-PACs show chemotaxis toward CXCL12, even though CXCR4 are mainly expressed in cytoplasm rather than on cell surface.

It was also revealed that canine DFs express CXCR4 at a functional level, which showed chemotactic response toward CXCL12. CXCR4 is expressed in murine fibroblasts and CXCR4 in murine fibroblasts responds to CXCL12 released from macrophages infiltrating skin injury, and activate the growth signal of fibroblasts (Nishimura *et al.*, 2012). Our results concur with the report in CXCR4 expression of

DFs. And it was suggested that DFs may home to the injury site through its migration ability toward CXCL12.

Although the similar expression manner of CXCR4 was observed between canine DFs and BM-PACs, BM-PACs showed chemotaxis at the lower concentration of CXCL12 than DFs. This result indicated that BM-PACs showed a higher functional expression of CXCR4 compared to DFs. Susceptibility to lower concentration of CXCL12 may contribute to increase the numbers of cells homing toward the injured site. Therefore, based on the findings in this chapter, it was suggested that BM-PACs administrated intravenously in subacute phase of SCI may migrate into the injured site according to the CXCR4-CXCR12 axis. It was also estimated that DFs shows homing ability because of the similar expression of CXCR4 and chemotaxis toward CXCL12, however, the effectiveness of cell migration toward the injured site may be lower when compared with BM-PACs.

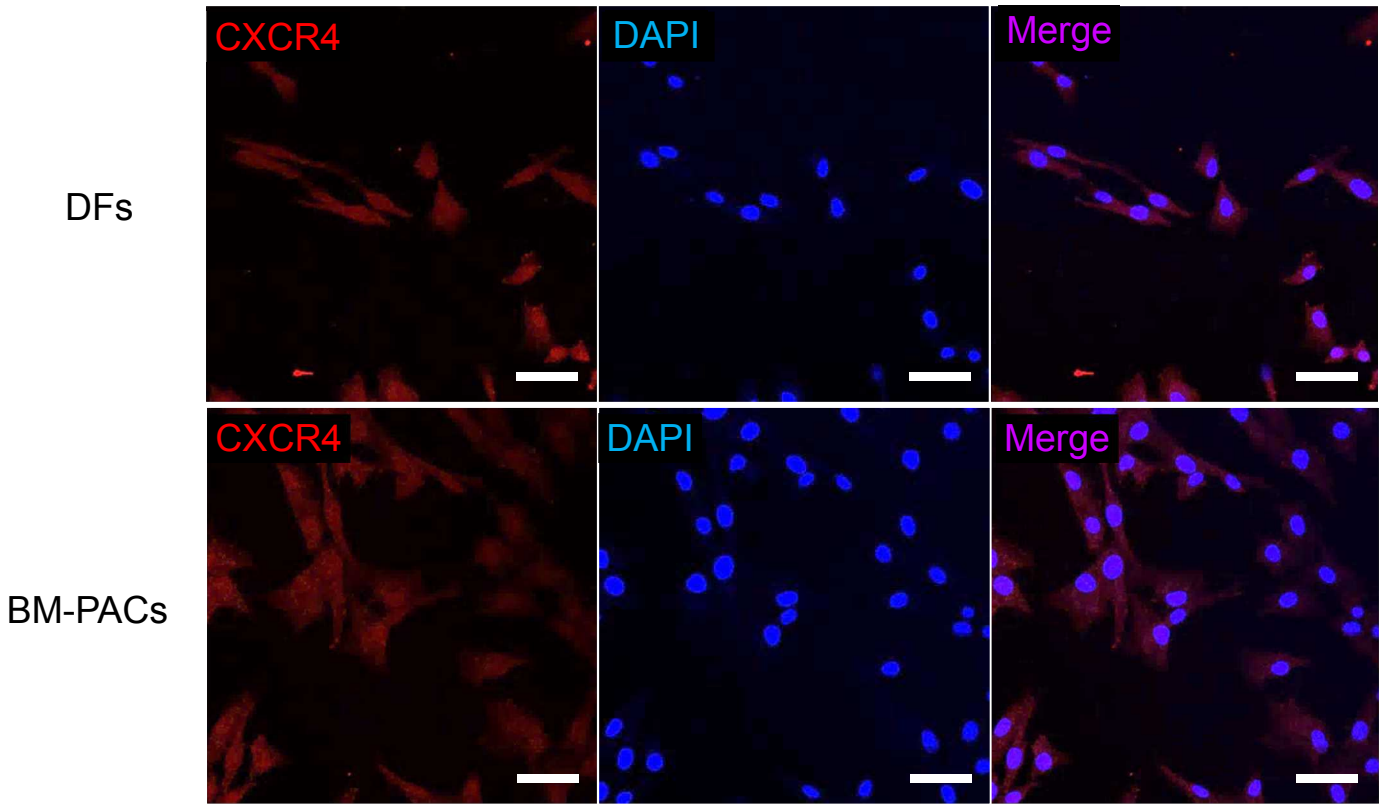

Fig. 1　Immunostaining of CXCR4 in DFs and BM-PACs

DFs and BM-PACs showed apparently positive expression of CXCR4 in the nuclei and cytoplasm.

Bars = 50 μm.

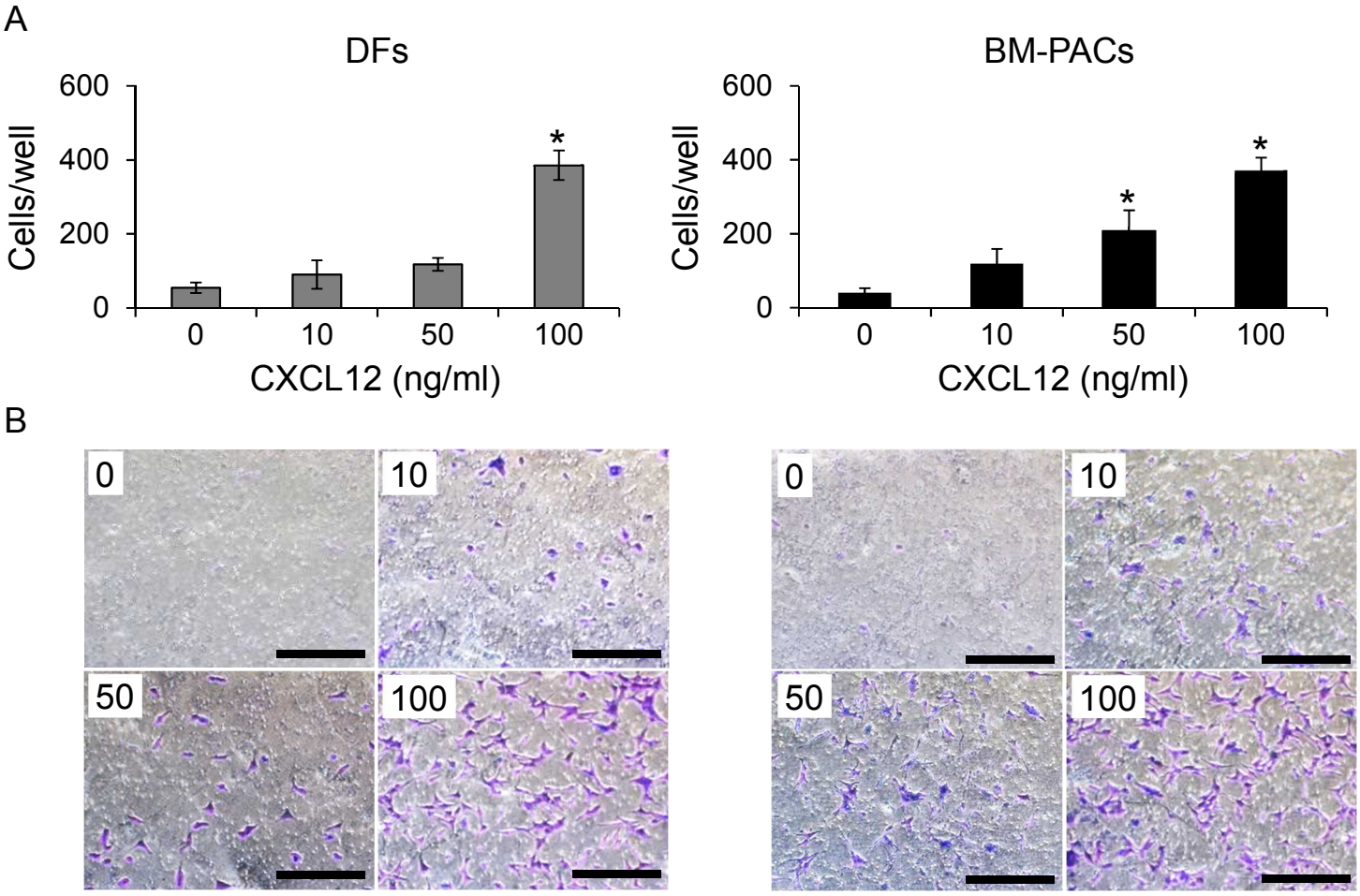

Fig. 2 Chemotaxis of DFs and BM-PACs toward CXCL12

Chemotaxis of DFs and BM-PACs was induced by different concentration of CXCL12 (0, 10, 50, and 100 ng/mL) for 24 hr using trans-well migration assay. *$P < 0.05$ compared to control (0 ng/mL, n = 3-4 for each group. (B) Representative images of migrated DFs and BM-PACs stained with crystal violet. Bars = 500 μm

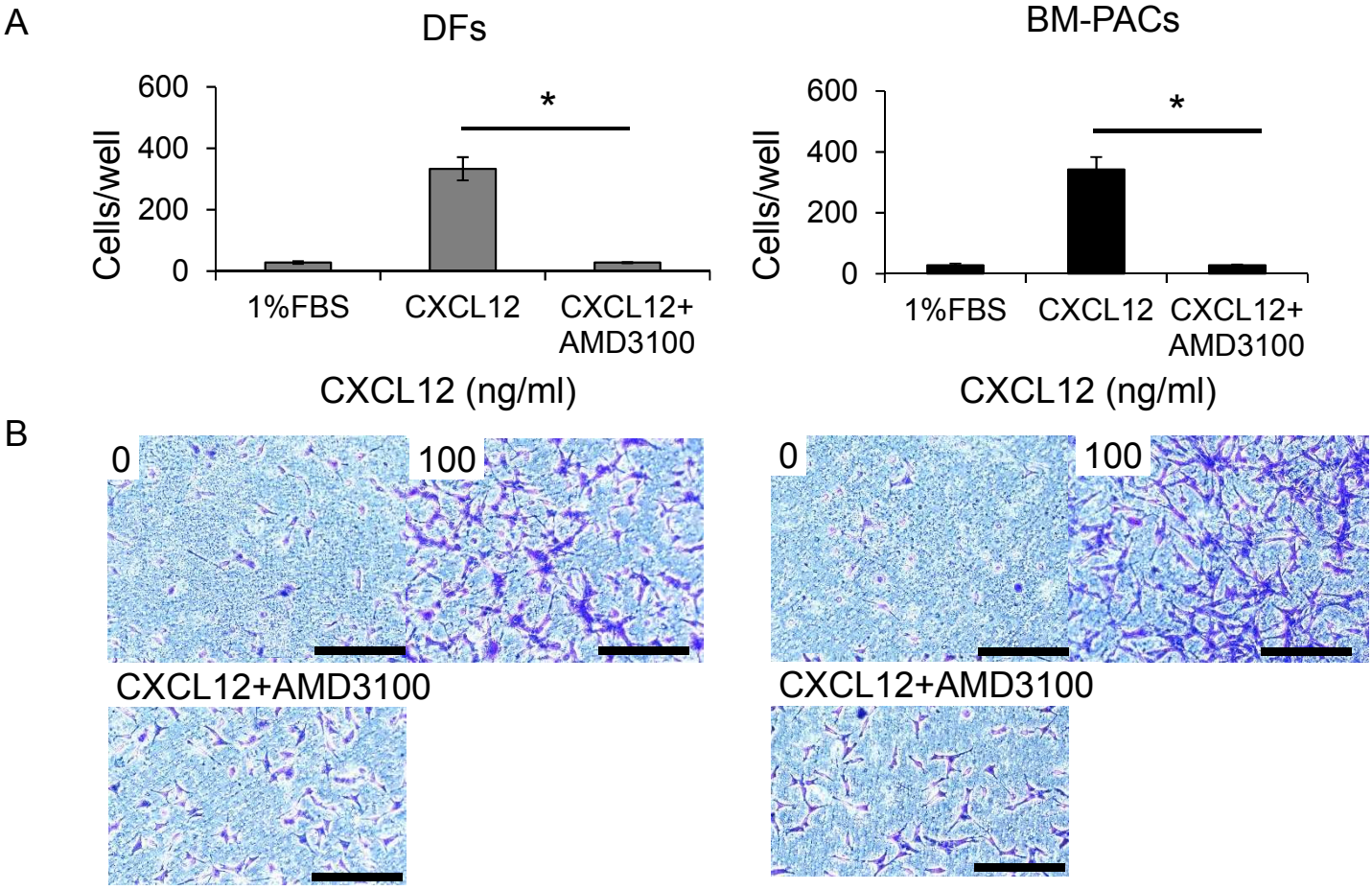

Fig. 3　Chemotaxis inhibition assay of DFs and BM-PACs toward CXCL12

Chemotaxis inhibition experiment of DFs and BM-PACs toward CXCL12 (100 ng/mL) were performed using CXCR4 antagonist (AMD3100). Chemotaxis of DFs and BM-PACs toward CXCL12 were blocked by AMD3100. *$P < 0.05$ compared to inhibitor group (CXCL12 100 ng/mL + AMD3100, n = 3-4 for each group. (B) Representative images of migrated DFs and BM-PACs stained with crystal violet.　Bars = 500 μm

Chapter2

Evaluation of trophic effects of BM-PACs

Introduction

In addition to homing ability, high trophic function of MSCs on the injured site is highly required achieve clinically effective outcome for regenerative therapy of SCI using MSCs by intravenous administration. In chapter 1, BM-PACs expressing CXCR4 showed chemoattractant property toward CXCL12 which upregulates in the damaged spinal cord in subacute phase of SCI. These results indicate the homing ability of BM-PACs. Therefore, the trophic function of BM-PACs by which contribute to tissue regeneration and protection was investigated in this data.

MSCs have been reported to exert trophic effects through secreting various growth factors such as neurotrophic and angiogenic factors (Chamberlain *et al.*, 2007). As I mentioned in general introduction, neurotrophic factors such as NGF and BDNF are reported to be released from MSCs and improve motor functional by protecting neurons from apoptosis which prolong motor neurons (Crigler *et al.*, 2006; Kim *et al.*, 2010; Sasaki *et al.*, 2009; Wilkins *et al.*, 2009). On the other hand, several kinds of angiogenic factors including VEGF, HGF, CTGF, and PDGF are reported to be released from transplanted MSCs and contribute to neovascularization in the injured spinal cord (Hsiao *et al.*, 2012; Hsieh *et al.*, 2013; Johnson *et al.*, 2013; Jing *et al.*, 2017). Reconstruction of blood supply is one of the most important factors for tissue

regeneration therefore, definition of effects brought by MSCs is important at developing an evidence-based cell therapy. The expression and secretion ability of these growth factors in human and murine MSCs have been enthusiastically investigated so far, however, there have been few reports which demonstrate whether and how canine MSCs have potential to supply these growth factors to the injured tissue.

The aim of this chapter is to investigate the trophic effects of BM-PACs. Gene expression levels of neural and angiogenic factors in BM-PACs were evaluated by comparing those of DFs. Secretion ability of the growth factors which showed significant gene expression was further detected using ELISA. Angiogenic ability was also examined by a tube formation assay using culture supernatant of BM-PACs and human umbilical vein endothelial cells (HUVEC).

Materials and Methods

BM-PACs and DFs

Canine BM-PACs and DFs which were isolated and cultured in same methods as Chapter 1 were used. Cryopreserved cells were thawed and cultured until cells reached over 80% confluency before use.

Real-time quantitative Polymerase Chain Reaction (qPCR)

Total RNA was isolated from BM-PACs and DFs using TRI reagent (Cosmo Bio, Tokyo, Japan) and complementary DNA was synthesized with ReverTra Ace qPCR RT master mix with gDNA Remover (Toyobo, Osaka, Japan). Real-time quantitative PCR (qPCR) assay was performed using SYBR Green (Thunderbird SYBR qPCR Mix; Toyobo, Osaka, Japan) to detect the gene expressions of NGF, BDNF, VEGF, HGF, PDGF, CTGF and FGF2. Increase of SYBR Green fluorescence was monitored by Step One Plus Real-Time PCR system (Applied Biosystems, Foster City, CA). Glyceraldehyde phosphate dehydrogenase (GAPDH) was used as an endogenous control gene. The primers used for qPCR are listed in Table1. Cycling conditions were 95℃ for 1 min and 40 cycles at 95℃ for 15 s, 60℃ for 1 min. Each sample was examined in triplicate. The copy numbers of each gene were calculated according to the values obtained from the standard curves.

VEGF ELISA

VEGF secretion ability of BM-PACs and DFs was measured using cell culture supernatant. BM-PACs and DFs were seeded into 12-well plate (Sumitomo Bakelite Co., Inc., Japan) at a density of 1×10^5 per well and incubated in DMEM contained 10% FBS. After 24 hr, culture medium were changed to DMEM contained 1% FBS at 37℃ in 5% CO_2 for 24 hr for starvation. Then, culture medium was changed to DMEM contained 1% FBS again and cells were incubated for another 24 hr. Culture supernatant was collected and centrifuged for 20 min at 1,000 g. Obtained supernatant were quickly cooled by liquid nitrogen and stored at -80℃ until use. Samples were gently thawed and VEGF concentration was determined using Canine VEGF Quantitative ELISA Kit (CAVE00, R&D Systems, McKinley Place, NM) according to supplier's protocol.

Tube formation assay

Tube formation assay was performed to determine the angiogenic function of VEGF secreted by BM-PACs and DFs. BM-PACs and DFs were cultured in DMEM contained 1% FBS and 1% antibiotics at a density of 2×10^5 per well in 12-well plate (Sumitomo Bakelite Co., Inc.) at 37℃ in 5% CO_2 for 18 hr and conditioned medium (CM) of

BM-PACs and DFs was prepared (BM-PACs-CM and DFs-CM). Passage 1 human umbilical vein endothelial cells (HUVEC, C2519A, Lonza, Japan) were seeded at a density of 1.4×10^4 per well in 96-well plate (Sumitomo Bakelite Co., Inc.) coated with growth factor reduced matrigel (356230, Falcon, Corning, Life Sciences, MA) and cultured in BM-PACs-CM, DFs-CM, DMEM contained 1% FBS and EGM-2 (basal medium for HUVEC) at 37℃ in 5% CO_2. To discriminate VEGF function, VEGF inhibitor (Cediranib:AZD2171, Selleck Chemicals, Houston, USA) was added to each medium. Vessel structures in three fields (×40) in each sample were examined after 18 hr using phase-contrast microscope. The number of tube and tube nods was counted, and covered area was measured using imaging software (Image J) to define angiogenic function. All samples were experimented in triplicate.

Statistical analysis

All data were expressed as mean ± standard division (SD). Comparisons were made by using One-way ANOVA with post hoc analysis (Dunnett's test) for multiple group comparison to detect statistical significance of the results. Comparisons between 2 groups were evaluated with the Student's t-test. Data management and statistical analyses were performed using EZR software package (Saitama Medical Center/Jichi

Medical University). Statistical significance of mean value of samples was accepted at $p < 0.05$.

Results

Gene expression of neurotrophic and angiogenic factors

Gene expression of VEGF, HGF, FGF-2, CTGF, and NGF was detected in BM-PACs and DFs. BDNF and PDGF expression was not detected in both cells. BM-PACs expressed significantly higher VEGF expression than those of DFs (Fig. 1-A). Based on the result of gene expression analysis, VEGF secretion ability was confirmed using ELISA and it was revealed that BM-PACs showed significantly higher secretion ability of VEGF than DFs (Fig. 1-B).

Functional validation of VEGF secreted from BM-PACs and DFs

To clarify the functional validity of VEGF secreted from BM-PACs and DFs, tube formation assay was performed using HUVECs. After cultured for 18 hr in BM-PACs-CM, the number of tubes and tube nodes, and the covering area significantly increased when compared with HUVECs cultured in DFs-CM and 1%FBS-DMEM. VEGF inhibitor inhibited these tube forming in any condition (BM-PACs-CM, DFs-CM, 1% FBS in DMEM, EGM-2) (Fig. 2).

Discussion

In this chapter, I investigated the expression of neurotrophic and angiogenic factors in BM-PACs by comparing with DFs. Although BDNF and PDGF expression were not detected, BM-PACs and DFs expressed the mRNA of NGF, VEGF, HGF, FGF2 and CTGF. This suggested that BM-PACs and DFs have the potential to contribute to tissue regeneration and protection through supplying these factors to the injured site. However, BM-PACs showed significantly higher expression of VEGF than DFs. Analysis using ELISA also revealed that BM-PACs actually released a significantly larger amount of VEGF protein than DFs. Among a variety of angiogenic factors, VEGF families are known as the most powerful modulators of vasculogenesis, angiogenesis and vascular maintenance (Ylä-Herttuala *et al.*, 2007). Therefore, it was suggested that BM-PACs have superior angiogenic property by releasing VEGF to the injured tissue at a high level when compared with DFs. However, it is hard to predict the absolute therapeutic effects from the gene expression level. Therefore, the actual function of VEGF secreted from BM-PACs was investigated by comparison with that of DFs in the next experiment.

To confirm and compare their angiogenic activity, the cell supernatant of BM-PACs and DFs were subjected to the angiogenesis bioassays *in vitro*. In accordance with the

results of ELISA, tube formation was significantly facilitated when HUVEC was cultured with BM-PACs-CM, when compared with DFs-CM and control medium. Although HUVEC shows tube formation in response to other cytokines such as HGF and endothelial growth factors (Xin *et al.*, 2001; Hsieh *et al.*, 2013), the effects of CM on tube formation was completely cancelled by adding the VEGF inhibitor. Therefore, angiogenic activity of BM-PACs predominantly depends on the secreted VEGF. Recent studies in human MSCs, the angiogenic effect of MSCs is almost determined by the expression levels of VEGF family (Imamura *et al.*, 2018; Hsiao *et al.*, 2012). Our results also indicate that the VEGF expression level closely correlate with the angiogenic effects of BM-PACs and DFs.

Angiogenesis is a critical element of the healing response to SCI and vasculature within the injured spinal cord remains in a state of active remodeling until at least 28 days post injury (Loy *et al.*, 2002; Popovich *et al.*, 1996). Therefore, BM-PACs may lead to tissue repair and are expected to improve functional outcome by promoting angiogenesis, when the cells migrate into and supply VEGF to the injured site in subacute phase of SCI.

In conclusion, BM-PACs have potential to promote neovascularization mainly through VEGF secretion and can be a suitable cell source for regenerative therapy for subacute

SCI. Taken together with the results in Chapter 1, it is hypothesized that BM-PACs administrated intravenously to subacute SCI can migrate into injured spinal cord through the CXCR4-CXCL12 axis and supply neurotrophic and angiogenic factors to the injured tissue. The high VEGF secretion level of BM-PACs may contribute to develop a novel regenerative therapy for SCI in dogs with scientific validity.

Primer	Sequence
BDNF forward	5’-AATCCCATGGGTTACACGAA-3’
BDNF reverse	5’-GCCAGCCAATTCTCTTTTTG-3’
NGF forward	5’-CAACAGGACTCACAGGAGCA-3’
NGF reverse	5’-ATGTTCACCTCTCCCAGCAC-3’
VEGF forward	5’-GCGCTGGTTTCTGTAGCGGTCA-3’
VEGF reverse	5’-CGAGGAAAGGGGAAGGGGCAAA-3’
HGF forward	5’-AAAGGAGATGAGAAACGCAAACAG-3’
HGF reverse	5’-GGCCTAGCAAGCTTCAGTAATACC-3’
PDGF forward	5’-CAACCGCAACGTGCAGTGCC-3’
PDGF reverse	5’-AACTCCCCGGGGTTCGGGTC-3’
CTGF forward	5’-TTTAGGAACAGTGGGAGAGC-3’
CTGF reverse	5’-CATGAAGAAGGCTGGAGAAC-3’
FGF2 forward	5’-CGATCCCCACGTCAAATTGCAA-3’
FGF2 reverse	5’-AATCGTTCAAAAAAGAAGCACTCGTCA-3’

Table. 1　Primers used for real-time qPCR reactions.

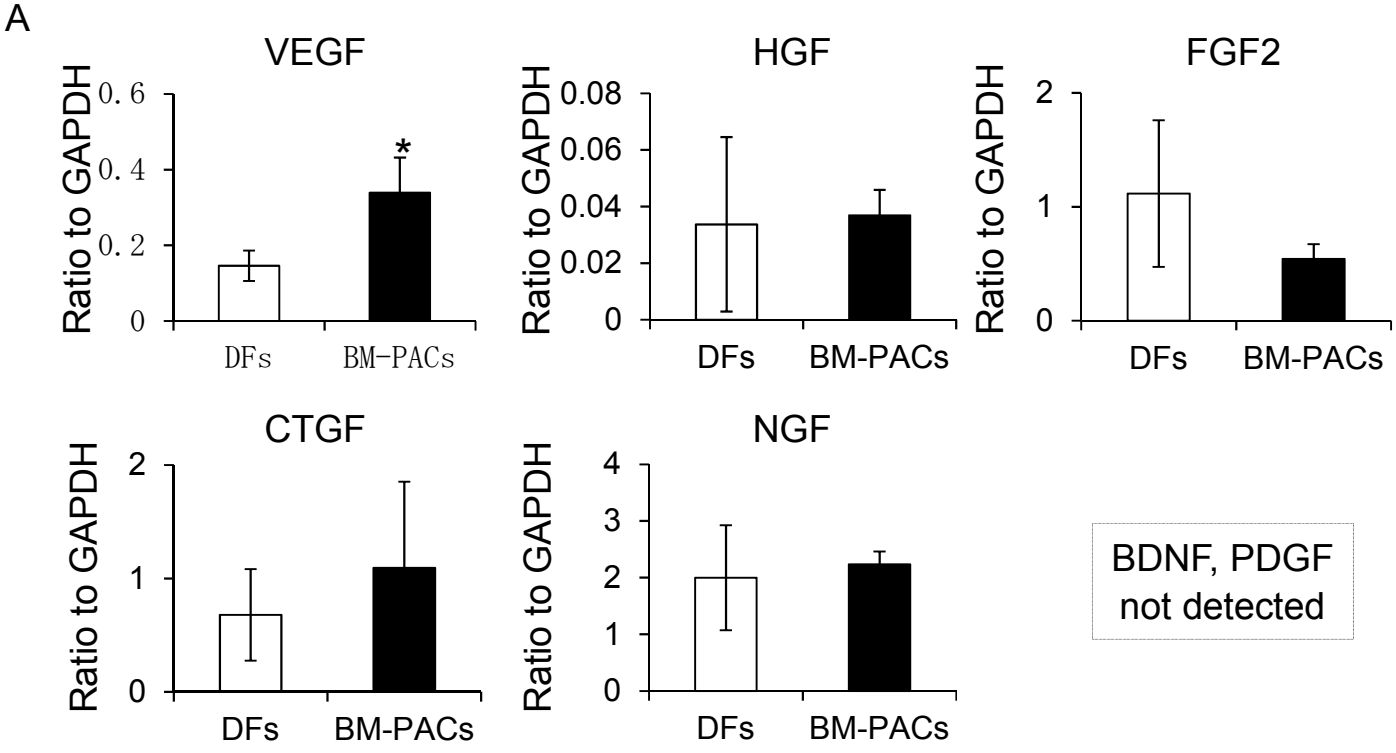

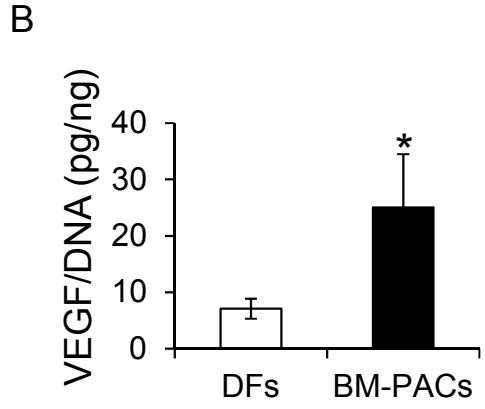

Fig. 1　Expression of angiogenic and neurotrophic factors in DFs and BM-PACs

(A) mRNA expression of VEGF, HGF, FGF2, CTGF and NGF. BM-PACs showed significantly higher VEGF expression than DFs mRNA of BDNF and PDGF was not detected.　* $P < 0.01$, n = 3 for each group.. (B) VEGF ELISA shows that BM-PACs secreted significantly larger amount of VEGF protein than DFs. *$P < 0.01$, n = 3 for each group.

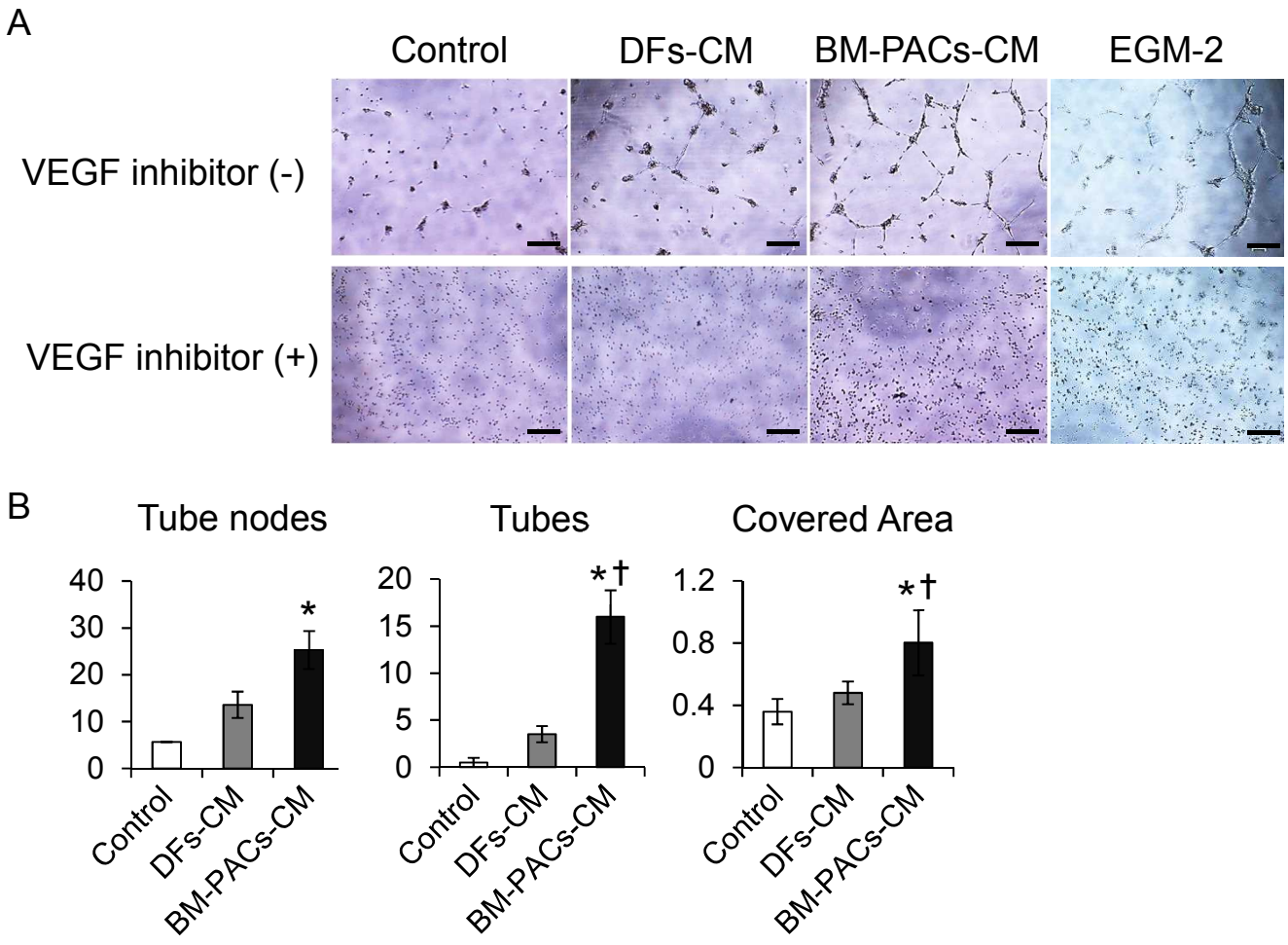

Fig. 2　Tube formation assay

(A) Representative pictures showing tube formation by HUVECs treated with 1% FBS in DMEM (control), DFs-CM, BM-PACs-CM, EGM-2 for 18 hr. Tube formation was inhibited by VEGF inhibitor under any condition (BM-PACs-CM, DFs-CM, 1% FBS in DMEM, EGM-2). (B) The numbers of tube nodes and tubes, and the covered area were examined using ImageJ software. BM-PACs-CM significantly induced the tube formation. The number of loops and the cell covered area was larger in BM-PACs-CM group than DFs-CM group. *, † $P < 0.01$ compared to control and DFs-CM group, respectively. n = 4 for each group. Bars = 200 μm.

Chapter 3

Therapeutic effects of intravenous administration of BM-PACs in a nude mouse model of subacute SCI

Introduction

In chapter 1, I demonstrated *in vitro* that BM-PACs have the potentials to home to the injured site according to CXCR4-CXCL12 axis which is involved in subacute phase of SCI. I also demonstrated *in vitro* in chapter 2 that BM-PACs have trophic effects to secrete various growth factors and angiogenic effects on injured spinal cord could be expected especially through VEGF. Taken together, it is hypothesized that intravenous administration of BM-PACs in patients with subacute SCI provides beneficial therapeutic effects through homing ability and trophic effects. It is essential to verify this hypothesis using a proper animal model to develop regenerative therapy using BM-PACs *in vivo*.

In this chapter, the effects of intravenous administration of BM-PACs were evaluated in a nude mouse subacute SCI model. Because subacute SCI in rodents were mostly defined as the period 1-2 weeks after SCI (Assinck *et al.*, 2017; Ide *et al.*, 2010; Kjell *et al.*, 2016), BM-PACs were intravenously administrated to the nude mice 10 days after induction of SCI. To delineate therapeutic effects of BM-PACs as MSCs, DFs were also administrated. Since DFs showed the chemotactic activity toward CXCL12 similar to BM-PACs and less angiogenic ability through releasing VEGF in Chapter 1, the impact of angiogenic potential of cells would be elucidate by comparing the therapeutic

outcomes between intravenous administration of BM-PACs and DFs. First, I evaluated cell distribution of BM-PACs and DFs after intravenous administration to nude mice of subacute SCI was observed. Then, the involvement of CXCR4-CXCL12 axis in homing of BM-PACs was also evaluated by an inhibition experiment using CXCR4 inhibitor (AMD3100). Therapeutic effects on functional and histological recovery were evaluated, and to what extent angiogenesis occurred at the injury site and contributed to these therapeutic effects was verified.

Materials and Methods

Animals

All animal experiments were approved by the Animal Care Committee of the Graduate School of Agricultural and Life Sciences, at the University of Tokyo (Approval No. P17-106). Eight-week-old female Balb/c nu/nu mice (n = 29, 18-23 g; Japan SLC, Shizuoka, Japan) were used to induce SCI and intravenous administration of canine BM-PACs. All surgical procedures were performed under general anesthesia with an inhalation of 2.5% isoflurane in oxygen.

BM-PACs and DFs

Canine BM-PACs and DFs cultured and cryopreserved in same methods as Chapter 1 was used. Cells were thawed and cultured until cells reached over 80% confluency before use.

Spinal cord injury model

Under general anesthesia, laminectomy was performed and severe contused SCI was induced at T10 level of vertebrae using Infinite Horizon (IH) impactor SCI device (Precision Systems & Instrumentation, Lexington, KY) at fore settings of 80

kdyn. Dura was kept intact and muscles and skins were sutured with 6-0 absorbable suture (Alfresa, Osaka, Japan). All mice were given water and food ad libitum and administrated 1 ml of lactated ringer's liquid (Fuso Pharmaceutical, Industries, Osaka, Japan) supplied with 5 mg/kg of enrofloxacin and 20 μg/kg of buprenorphine (Otsuka Pharmaceutical, Tokushima, Japan) by subcutaneous injection twice a day for 2 weeks. Manual bladder expression was also performed twice a day until recovery of the bladder reflex was confirmed.

Evaluation of functional recovery

Functional recovery was evaluated once a week for 6 weeks after cell administration using Basso Mouse Scale (BMS) (Table 3-1, Basso et al, 2006). Based on the video recorded gait, the average scores by two assessors blinded to the treatment groups were adopted.

Cell administration and tracking

Cells were fluorescence-labeled with vivo track 680 (Perkin Elmer, Norwalk, CT) and 100 μl of cell suspension (1×10^6 cells/μl in DMEM) was injected from femoral vein using 30-gauge low dose insulin syringe (Becton Dickinson, Franklin Lakes, NJ,

USA) in the subacute phase of SCI (10 days after injury) under general anesthesia. For control group, medium of the same volume was injected. The distribution of transplanted cells was tracked using In Vivo Imaging System (IVIS, Summit Pharmaceuticals International, Tokyo, Japan) within 1 hr after administration. Cell tracking was also performed after 1 day of cell administration and once a week for 6 weeks. The base line of the fluorescence intensity was adjusted at the maximum intensity with which no apparent signal was observed in the control group. To define to what extent the CXCR4-CXCL12 axis involved in homing of BM-PACs to the injury sites, a part of mice were administrated BM-PACs conditionally treated with CXCR4 inhibitor (AMD3100) as described in Chapter 2. Three mice in each group was euthanatized 1 week after administration, and injured spinal cord and other organs including heart, lung, kidney and spleen were collected to directly determine the cell migration into each organ. The signal intensity observed in the injured spinal cord was measured as radiant efficiency using (IVIS software). Other animals were euthanatized after 6 weeks and the injured spinal cord was collected for histological evaluation.

Tissue processing

After 6 weeks of observation period, mice were euthanatized and immediately perfused with 4% paraformaldehyde (PFA). Spinal cord stumps 1 mm-long both rostral and caudal from the lesion epicenter was collected and placed in 4% PFA for overnight. Samples were dehydrated by 20% and 30 % sucrose fluid, and frozen-embedded with OCT compound (Tissue-TeK® O.C.T compound, Sakura Fine-tek, Japan). Serial transverse sections were obtained at 20-μm thickness using a cryotome (Laica, Deerfield, IL, USA) and slides were frozen until use.

Luxol Fast Blue (LFB) staining

LFB staining was performed to determine the remaining white matter and microphotographs of stained area in serial cross sections 200 μm apart rostrally and caudally from the lesion epicenter was obtained by phase-contrast microscope. LFB positive area was measured using Image J software.

Immunohistochemistry

Tissue slides were washed with TBS-T three times for 5 min each. After washing, tissue slides were blocked with TBS-T containing 10% NGS and incubated for 1 hr at room temperature. After blocking, rabbit polyclonal anti-CD31 (1:50, ab28364,

Abcam) was applied on tissue slides as primary antibody. Slides were incubated overnight at 4℃. After incubation, slides were washed with TBS-T three times for 5 min each and incubated with HRP labeled polymer (K4003, Dako, Tokyo) for 1 hr at room temperature. Finally, sections were washed with TBS-T three times for 5 min each and diaminobenzidine (DAB) substrate (K3468, Dako) was applied. Microphotographs of stained area in serial cross sections 200 μm apart rostrally and caudally from the lesion epicenter was obtained by a phase-contrast microscope. The CD31 positive area of dorsal white matter was quantitatively measured using Image J software.

To determine the axons in the injured area, fluorescent immunohistochemistry was also performed using rabbit anti-NF200 (1:400, N4142, Sigma Aldrich, St. Louis, MO). Further, to discriminate whether axonal regrowth contributed to the axonal sparing, another set of slides were incubated with chicken polyclonal anti-NF200 (1:1000, ab134459, Abcam) and rabbit polyclonal anti-GAP43 (1:500, ab16053, Abcam). After blocked with TBS-T containing 10% NGS, the primary antibodies were applied on the slides and incubated overnight at 4℃. Alexaflour 568 goat pAb to chicken IgG (1:400, ab175711, Abcam), Alexaflour 488 goat pAb to rabbit IgG (1:400, ab150081, Abcam) were used as secondary antibodies and incubated at room temperature for 1 hr. Nuclei were counterstained with DAPI (1:1000) and slides were washed with TBS-T three

times for 5 min each. Specimens were mounted with an antifade mount (Prolong Gold, Invitrogen) and microphotographs were observed with a confocal microscope (Carl Zeiss). The area positive for NF200 in serial cross sections 200 μm apart rostrally and caudally from the lesion epicenter was quantitatively measured using Image J software. NF200 and GAP43 co-stained area at the lesion epicenter were also measured from five randomly selected fields of dorsal column of spinal cord.

Statistical analysis

All data were expressed as mean ± standard division (SD). Comparisons were made by using One-way ANOVA with Dunnett's test for multiple group comparison to detect statistical significance of the results. Comparisons between 2 groups were evaluated with the Student's t-test. Data management and statistical analyses were performed using EZR software package. Statistical significance of mean value of samples were accepted at $p < 0.05$.

Results

Functional recovery after IV administration of BM-PACs and DFs

Functional recovery was evaluated using BMS score for 6 weeks after IV administration (Fig. 1). All mice lost the ability to walk after contused injury and BMS score in control group was not recovered during 6 week of observation period. DFs group showed mild recovery after intravenous administration, but there were no statistical differences in functional recovery between DFs and control group. On the other hand, significantly higher functional recovery than control group was observed in BM-PACs group. The functional recovery in BM-PACs group was observed mainly at the early period after cell administration and significantly higher BMS score than DFs group was also recorded 2-3 weeks after SCI. During the observation period, mice in BM-PACs group gradually recovered and the final BMS scored 4 on the average, which indicates the animals occasionally shows voluntary walking ability with weight bearing.

Distribution of intravenously administrated BM-PACs and DFs

Immediately after administration, the fluorescent signals were detected mainly in the lung, then, those signals became more apparent around the injured site from 1 day after administration. The highest signals around the injured site were observed

after 1-2 weeks in both groups. These signals gradually attenuated after 2 weeks and were not detected after 4 weeks (Fig. 2A). Fluorescent signals were also observed in the collected tissues the injured spinal cord and the other normal organs (Fig. 2B). No significant difference in signal intensity was observed between DFs and BM-PACs group. The signal intensity at the lesion of the spinal cord 1 week after administration of BM-PACs was significantly decreased by the pretreatment with CXCR4 inhibitor (Fig. 2C).

Angiogenesis in the injured spinal cord after IV administration of BM-PACs and DFs

BM-PACs group had larger CD31-positive area than DFs and control group. Significant differences were observed not only at the lesion epicenter but also around the lesion site rostral and caudal to the epicenter. No significant differences were observed between DFs and control group (Fig. 3).

Axonal sparing and regeneration in the injured spinal cord after IV administration of BM-PACs and DFs

Quantification of LFB-positive area revealed significant differences between BM-PACs and control groups not only at the lesion epicenter but also around the lesion

site, especially in caudal site. DFs group showed a tendency to have more LFB-positive area than control group and significant differences were observed at 800-μm rostral to the epicenter (Fig. 4).

BM-PACs group also had a tendency to have a larger NF200 positive area than other groups. However, significantly larger NF200-positive area was only observed at 600-μm caudal site to the lesion epicenter. On the other hand, DFs groups showed no apparent increase in NF200-positive area and there was no significant difference between control group (Fig. 5).

NF200-positive axons co-stained with GAP43 significantly increased in BM-PACs group when compared with other groups. No significant difference was observed between DFs and control group (Fig. 6).

Discussion

In this chapter, I investigated *in vivo* homing ability and therapeutic effects of BM-PACs intravenously administrated to a subacute SCI model in nude mice. Therapeutic effects were evaluated by locomotion recovery and histological examination of injured spinal cord focusing on the angiogenesis and axonal regeneration. A comparative approach with DFs which showed similar homing ability through CXCR4-CXCL12 axis and less angiogenic ability in vitro was applied.

Significant functional recovery following to homing of cells was observed only in BM-PACs group. The functional recovery continued in BM-PACs group even after the fluorescent signal attenuated and disappeared, while that was limited in DFs group. These immediate and sustainable therapeutic effects by BM-PACs suggested that BM-PACs contributed to not only protection of injured cells but also tissue regeneration probably through the trophic effect.

Cell tracking using IVIS revealed that both BM-PACs and DFs showed similar distribution after intravenous administration. Immediately after the administration, fluorescent signals were mostly detected in the lungs. It is well known that systemically administrated human MSCs are once entrapped within the lungs due to arrest by the capillaries, and then migrates out from lung to organs such as spleen and liver

(Luminita *et al.*, 2018). Actually, fluorescent signals of DFs and BM-PACs were detected in the other organs such as heart and kidney. It was suggested that these cells traveled in the blood to whole body tissues. The fluorescent signals were also detected in the spinal cord, however those were confined in the lesion area. Fluorescent signal intensity of BM-PACs in the spinal cord lesion at 1 week after administration was significantly decreased by pretreatment with CXCR4 inhibitor. This suggested that CXCR4-CXCL12 axis is significantly involved in the mechanism of homing of BM-PACs into the spinal cord lesion in subacute phase. Based on the signal intensity in the lesion site, it was also demonstrated that almost the same number of cells homed to the injured spinal cord in BM-PACs and DFs groups. This similarity was accountable by the results described in Chapter 1 that BM-PACs and DFs showed comparative CXCR4 expression and chemoattractant property toward CXCL12 in vitro.

The signal intensity in the lesion site peaked at 1-2 weeks and became undetectable 4 weeks after BM-PACs and DFs administration. It has been reported that human MSCs systemically administrated to healthy immunodeficiency mice were also detectable in the lungs, livers, spleens and kidneys, and no longer detectable after 2-3 weeks by bioluminescence imaging (Kid *et al.*, 2009). In other studies, the life span of

transplanted human and rodent MSCs to injured tissue were also reported to be a few weeks (Mooney *et al.*, 2008; Daley *et al.*, 2008).

The underlying mechanism of the therapeutic effects by transplanted BM-PACs was investigated by histological analysis focusing on angiogenesis. The significant larger area positive for CD31 in BM-PACs group suggested that the trophic effect of BM-PACs greatly contributed to angiogenesis of the injured spinal cord. On the other hand, DFs failed to show angiogenic effect, even though the numbers of cells homed to the lesion site was mostly equal to BM-PACs. Thus, the differences in the trophic effects between BM-PACs and DFs may have contributed to the difference in the angiogenic outcome. VEGF is the most possible candidate involved in the trophic effect induced by BM-PACs, because, as shown in Chapter 2, its expression and secretion were significantly higher in BM-PACs than in DFs, while the expression levels of other angiogenic factors including HGF and FGF2 were comparable.

Intravenous administration of BM-PACs eventually contributed to increase in myelinated white matter. Although significant difference between DFs and control group was limited at 600 μm caudal to the epicenter, BM-PACs group tended to have more NF200 positive area around the lesion. These neuroprotective effects might come from other neuroprotective trophic factors rather than VEGF. However, it is reported

that VEGF directly supplied to injured spinal cord contributed to not only angiogenesis but also neuroprotective property (Park *et al.*, 2010). Therefore, there was a possibility that the protective effects on myelin and axon were also induced by VEGF secreted from BM-PACs.

The significant increase in axons co-stained with NF-200 and GFP43 at the dorsal funiculi of the injured spinal cord was observed in BM-PACs group. Co-staining of NF-200 and GAP43 allows the visualization of the process of axonal regeneration, thus this result verified intravenous administration of BM-PACs contributed to axonal regeneration after SCI. The corticospinal tract (CST) runs through the dorsal funiculi in rodent spinal cord and highly synapses to the motor neurons (Bareyre *et al.*, 2005; Bieler *et al.*, 2018). Therefore, axonal regrowth in the dorsal funiculi was thought to have greatly contributed to motor functional recovery in BM-PACs group. Although direct relationship between angiogenesis and axonal regrowth was not investigated in this study, it is reported that prostacyclin known as a vasodilation factor derived from endothelial cells induced axonal regrowth in CST after experimental myelitis (Muramatsu *et al.*, 2012). Therefore, it was suggested that the remarkable angiogenesis induced by BM-PACs eventually contributed to increase in blood supply and axonal regeneration after SCI.

In conclusion, in this chapter I revealed that intravenously administrated BM-PACs successfully homed into injured spinal cord in subacute phase of SCI. The CXCR4-CXCL12 axis was shown to be significantly involved in the mechanism of *in vivo* homing ability of BM-PACs. It was also verified that therapeutic effects were achieved by intravenous administration of BM-PACs. With comparing the functional and histological outcome between BM-PACs and DFs group, it was suggested that BM-PACs homed to the injured site exerted therapeutic effects mainly by the angiogenic ability. Although trophic effect of BM-PACs through VEGF secretion to the injured spinal cord was certainly involved to promote angiogenesis, further investigation using BM-PACs suppressed VEGF expression should be performed to delineate to what extent VEGF secreted from BM-PACs contributed to the therapeutic effect. However, the outcomes obtained in this chapter may contribute to develop an evidence-based regenerative therapy for canine SCI. Although the safety of intravenous administration of BM-PACs should be evaluated prior to clinical application, intravenous administration of BM-PACs is expected to be a novel therapeutic strategy for dogs with severe SCI in subacute phase.

Score	
0	No ankle movement
1	Slight ankle movement
2	Extensive ankle movement
3	Plantar placing of the paw with or without weight support -or- Occasional, frequent or consistent dorsal stepping but no plantar stepping
4	Occasional plantar stepping
5	Frequent or consistent plantar stepping, no coordination -or- Frequent or consistent plantar stepping, *some* coordination, paws *rotated* at initial contact and lift off (R/R)
6	Frequent or consistent plantar stepping, *some* coordination, paws *parallel* at initial contact (P/R, P/P) -or- Frequent or consistent plantar stepping, *mostly* coordinated, paws *rotated* at initial contact and lift off (R/R)
7	Frequent or consistent plantar stepping, *mostly* coordinated, paws *parallel* at initial contact and *rotated* at lift off (P/R) –or- Frequent or consistent plantar stepping, *mostly* coordinated, paws *parallel* at initial contact and lift off (P/P), and *severe* trunk instability
8	Frequent or consistent plantar stepping, *mostly* coordinated, paws *parallel* at initial contact and lift off (P/P), and *mild* trunk instability –or- Frequent or consistent plantar stepping, *mostly* coordinated, paws *parallel* at initial contact and lift off (P/P), and *normal* trunk stability and tail *down or up* & *down*
9	Frequent or consistent plantar stepping, *mostly* coordinated, paws *parallel* at initial contact and lift off (P/P), and *normal* trunk stability and tail *always* up.

Table 3-1. Scores and operational definitions for the basso mouse scale for locomotion (BMS)

Slight: Moves less than half of the ankle joint excursion.

Extensive: Moves more than half of the ankle joint excursion.

Plantar placing: Paw is actively placed with both the thumb and the last toe of the paw touching the ground.

Weight support: (dorsal or plantar): The hindquarters must be elevated enough that the hind end near the base of the tail is raised off of the surface and the knees do not touch the ground during the step cycle.

Stepping: (dorsal or plantar): Weight support at lift off, forward limb advancement and re-establishment of weight support at initial contact.

Occasional: Stepping less than or equal to half of the time moving forward.

Frequent: Stepping more than half the time moving forward.

Consistent: Plantar stepping all of the time moving forward with less than 5 missed steps (due to medial placement at initial contact, butt down, knee down, skiing, scoliosis, spasms or dragging) or dorsal steps.

Coordination: For every forelimb step a hindlimb step is taken and the hindlimbs alternate during an assessable pass. For a pass to be assessable, a mouse must move at a consistent speed and a distance of at least 3 body lengths. Short or halting bouts are not assessable for coordination. At least 3 assessable passes must occur in order to evaluate coordination. If less than 3 passes occur then the mouse is scored as having no coordination.

Some coordination: Of all assessable passes (a minimum of 3), most of them are *not* coordinated.

Most coordination: Of all assessable passes (a minimum of 3), most of them *are* coordinated.

Paw position: *Digits* of the paw are parallel to the body (P), turned out away from the body (external rotation: E) or turned inward toward midline (internal rotation; I).

Severe trunk instability: Severe trunk instability occurs in two ways.

(1) The hindquarters show severe postural deficits such as extreme lean, pronounced waddle and/or near collapse of the hindquarters predominantly during the test. –or-

(2) Five or more of any of the following *events* stop stepping of one or both hindlimbs

• Haunch hit: the side of hindquarters rapidly contacts the ground

• Spasms: sustained muscle contraction of the hindlimb which appears to immobilize the limb in a flexed or extended position

• Scoliosis: lateral deviation of the spinal column to appear "C" shaped instead of straight

Mild trunk instability: Less than 5 events listed above and some sway in the hindquarters. Mild trunk instability is scored when the pelvis and haunches predominantly dip, rock, or tilt from side-to-side (tilt). If the tail is up, the swaying of the pelvis and/or haunches produces side-to-side movements of the distal third of the tail which also indicates mild trunk instability (side tail).

Normal trunk stability: No lean or sway of the trunk, and the distal third of the tail is steady and unwavering during locomotion.

No severe postural deficits or events and less than 5 instances of mild instability.

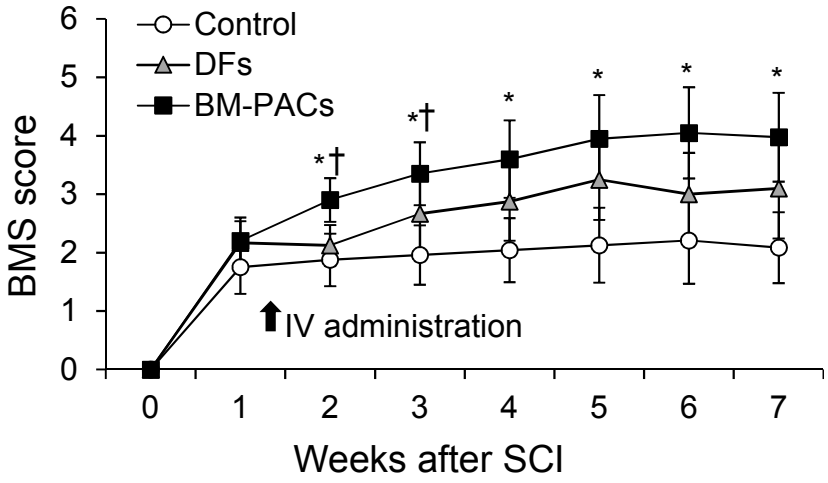

Fig. 1　BMS analysis for locomotive recovery

The graph shows locomotive recovery of SCI mice intravenously administrated medium (control), DFs and BM-PACs at 10 days after the induction of SCI. BM-PACs group showed significantly higher BMS scores than control and DFs group after 2 -3 weeks post SCI. Significantly higher BMS scores than control groups were also recorded in BM-PACs group, but not in DFs group. Mice in BM-PACs groups gradually recovered and final BMS score reached at 4 (occasional planter stepping) on the average. $*P < 0.05$ compared to control, $\dagger P < 0.05$ compared to DFs, n = 5-6 for each group.

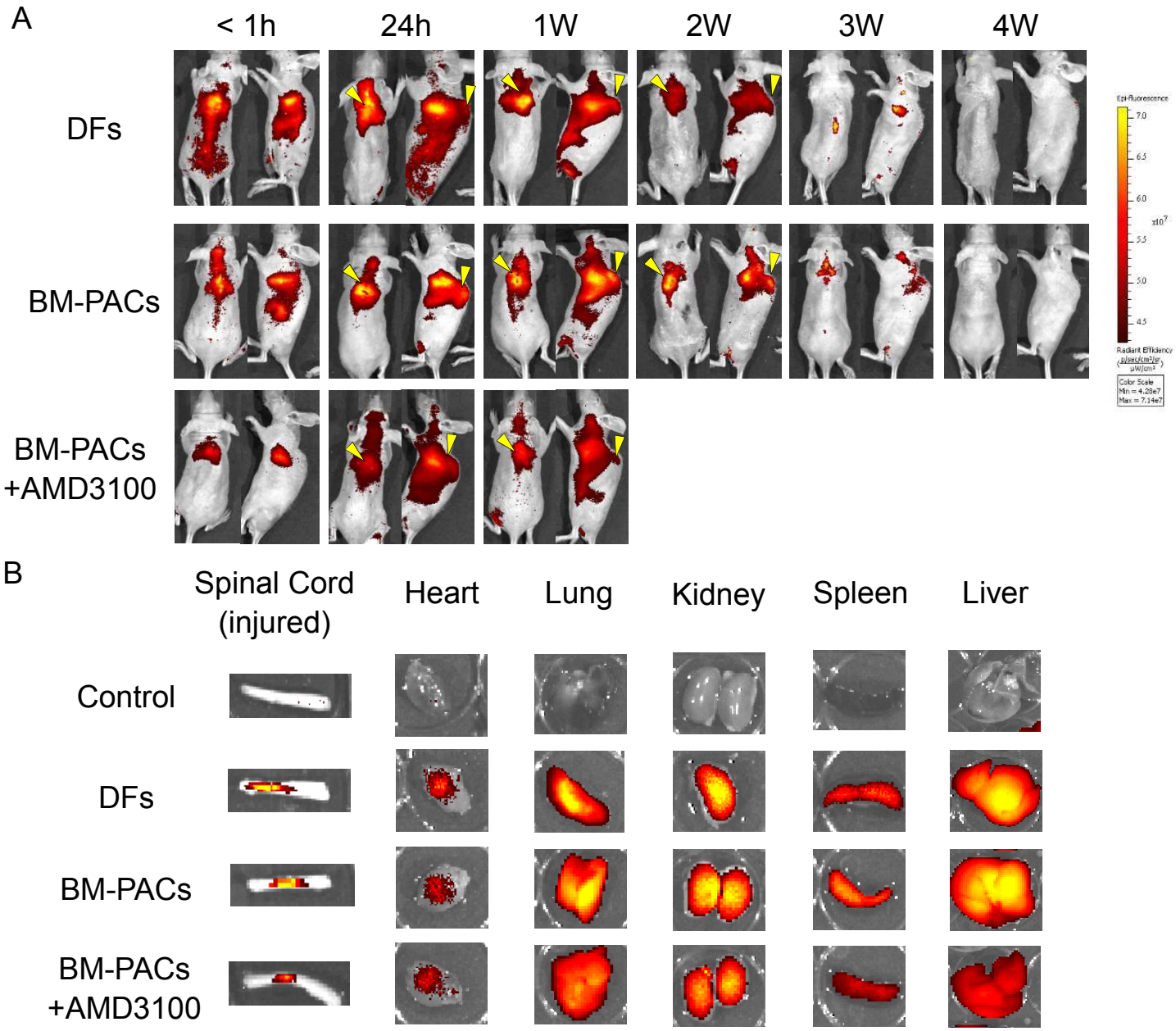

Fig. 2　Distribution of cells labelled with vivo track 680 after intravenous administration.

(A) Optical imaging of mice after 0-4 weeks of intravenous cell administration was taken at dorsoventral and lateral position. Note that higher fluorescent intensity is observed around the injured spinal cord (yellow arrow head). These signal intensity was prominent the next day after administration and peaked at 1 week, and detectable up to 2 weeks. (B) Detection of fluorescent signals in the organs resected after 1 week of cell administration.

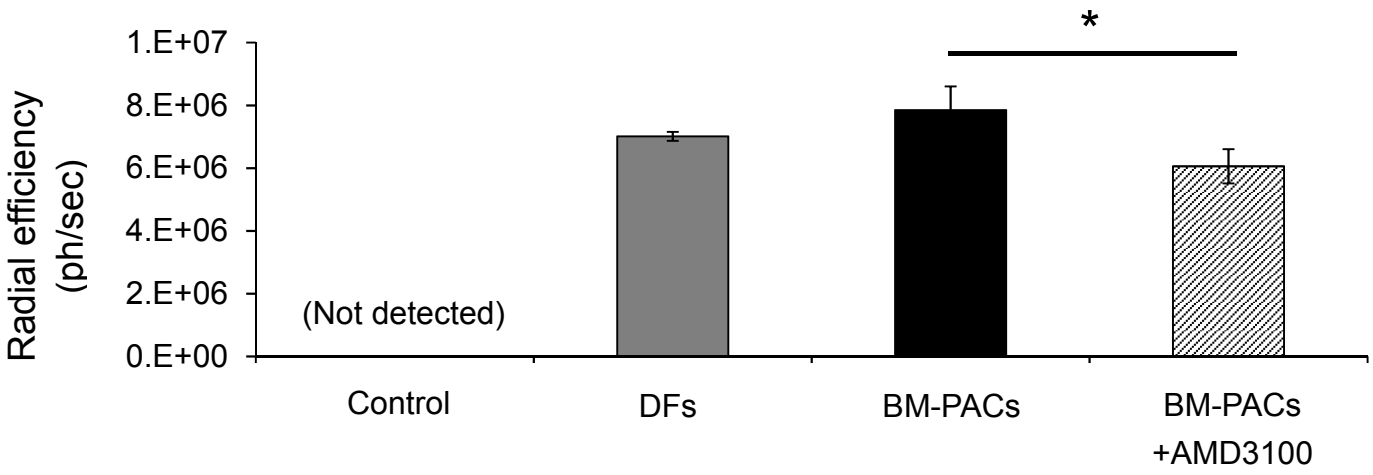

(C) The signal intensity at the lesion of the resected spinal cord after 1 week of cell administration was quantified. No significant difference was found between DFs and BM-PACs group. However, the signal intensity at the lesion site of BM-PACs group was significantly decreased by the pretreatment with CXCR4 inhibitor. n = 3 for each group. *, † $P < 0.01$ BM-PACs group compared to CXCR4 inhibitor group.

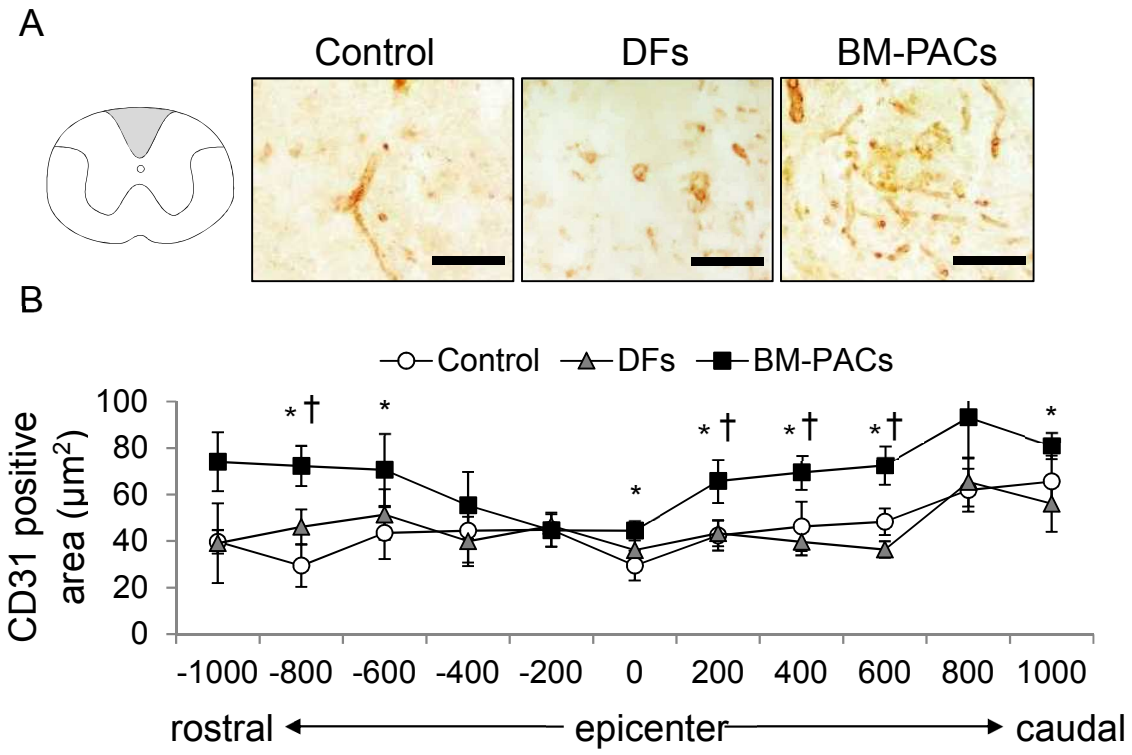

Fig. 3 CD31 expression in the injured spinal cord after 6 weeks of IV administration

(A) The scheme indicates the representative images of vessels stained with CD31. (B) The CD31 positive area in the dorsal funiculi (grey area in the scheme) 1 mm rostral and caudal to the epicenter was measured. IV administration of BM-PACs induced significant increase of CD31 positive area compared to DFs and control group not only at but also around the lesion epicenter. There was no statistical significance between DFs and control group. **P* < 0.05, BM-PACs compared to control; †P < 0.05, BM-PACs compared to DFs, n = 3-4 for each group. Bars = 100 μm.

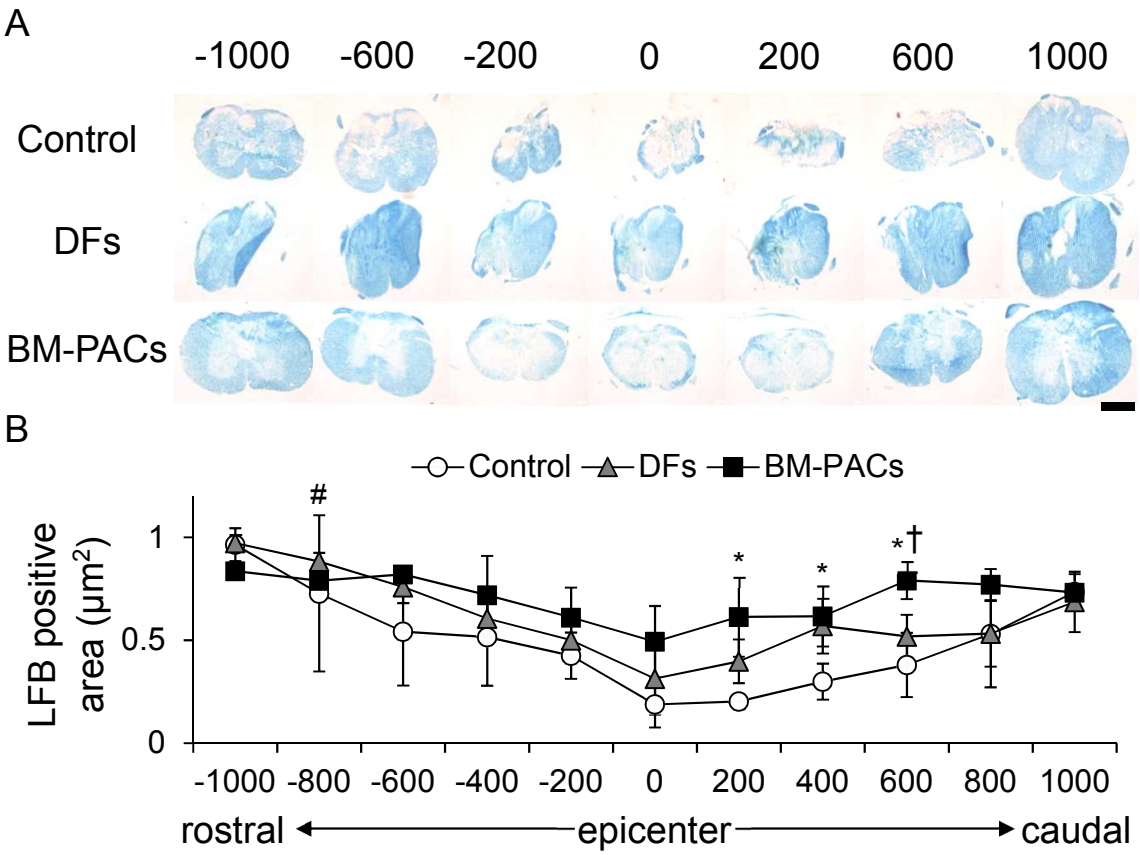

Fig. 4　LFB staining of injured spinal cord 6 weeks after each intervention
(A) Representative images of LFB staining of serial sections 1,000 μm rostral and caudal to the epicenter.　(B) Quantification of the LFB positive myelinated area. LFB positive area was significantly increased at the caudal area in BM-PACs group compared to control and DFs group. A significant difference was also observed between DFs and control group at 800 μm rostral to the epicenter.　*$P < 0.05$, BM-PACs compared to control; †$P < 0.05$, BM-PACs compared to DFs, #$P < 0.05$, DFs compared to control, n = 3-4 for each group. Bars = 500 μm.

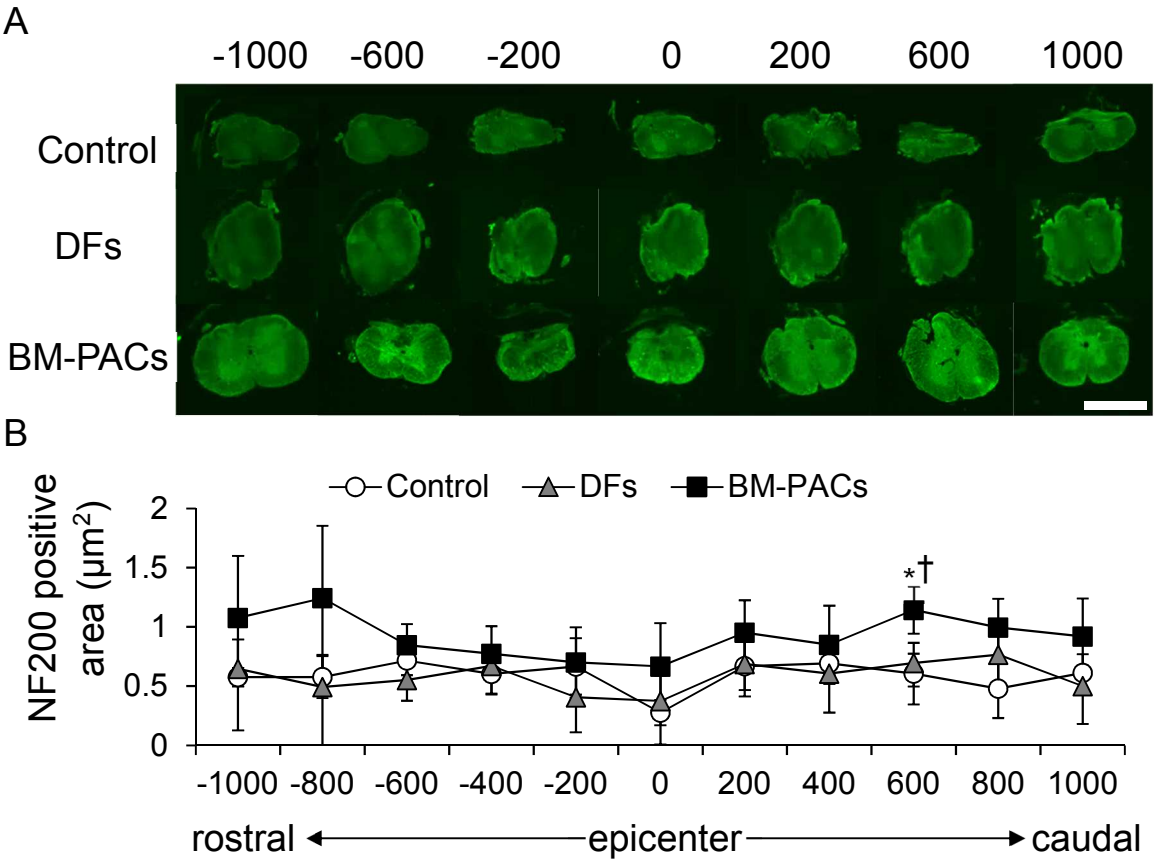

Fig. 5 Immunohistochemistry for NF200 of injured spinal cord after each intervention

(A) Representative images of NF200 staining of serial sections 1,000 μm rostral and caudal to the epicenter. (B) Quantification of the NF200 positive axonal area. NF200 positive area in BM-PACs group was significantly increased at 800 μm caudal to the epicenter compared to DFs and control group. $*P < 0.05$, compared to control, , $\dagger P < 0.05$, compared to DFs, n = 3-4 for each group. Bars = 500 μm.

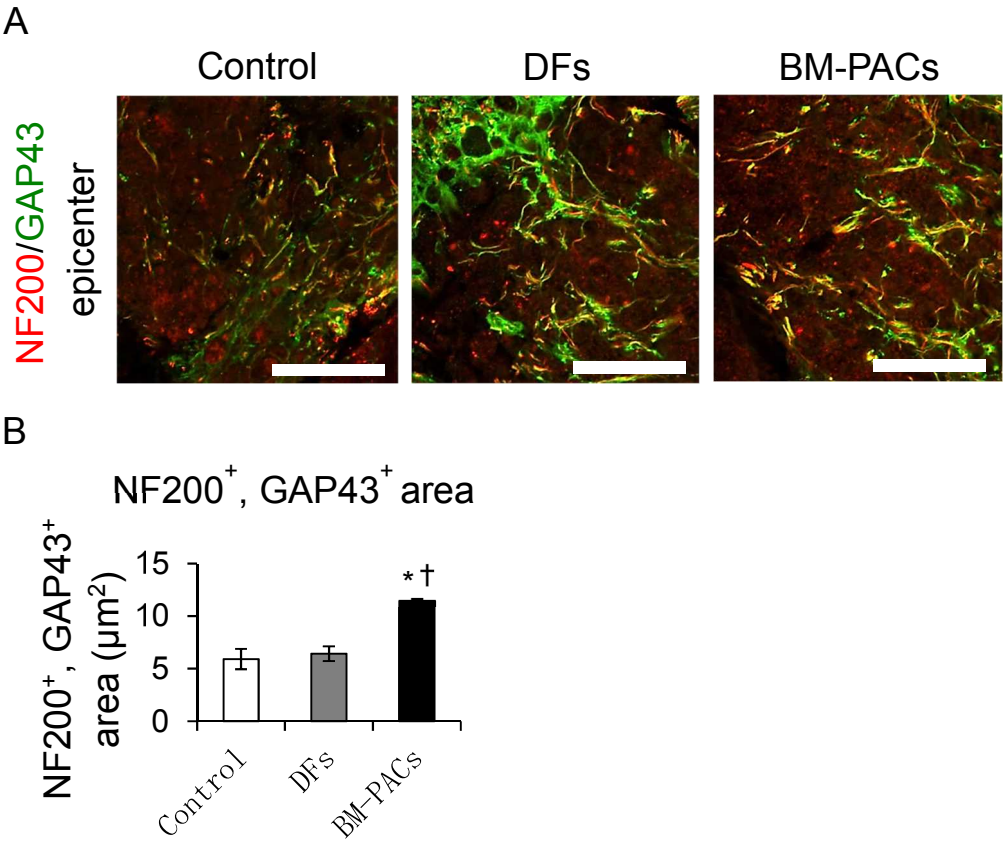

Fig. 6　Co-staining of NF200 and GAP43 of injured spinal cord after each intervention.

(A) Axons co-expressed NF200 (red) and regeneration-associated marker GAP43 (green) were apparently increased at the epicenter and caudal side of dorsal white matter in BM-PACs group compared to control and DFs group. (B) Quantitative analysis of merged area (yellow) show BM-PACs administration significantly increases GAP43 expression in axons at the epicenter of injured spinal cord.　*$P < 0.05$, compared to control, , †$P < 0.05$, compared to DFs, n = 3 for each group. Bars = 50 μm.

Chapter 4

Safety of intravenous administration of BM-PACs in dogs and development of a clinical evaluation method of homing effects of BM-PACs

Introduction

In chapter 3, I have demonstrated that intravenous administration of BM-PACs in mice with subacute SCI induces significant locomotion recovery. It is expected that BM-PACs home to the injured spinal cord and exert trophic effects promoting angiogenesis, which leads tissue protection and regeneration. These results revealed the efficacy of intravenous administration of BM-PACs and the possible mechanism has been verified, however the safety of intravenous administration of BM-PACs in dogs is unclear. Generally, cell-based therapy using systemic administration has a risk of pulmonary embolism. The risk of systemic administration supposed to increase depending on the number of cells and may cause sudden death in the worst case (Furlani *et al.*, 2009). Based on the results in Chapter 3, BM-PACs were trapped in the lung immediately after intravenous administration. Therefore, it is essential to confirm whether intravenous administration of BM-PACs results in serious complications caused by pulmonary embolism or not to develop a clinically safe regenerative therapy.

Another major risk reported in cell-based therapies in human medicine is anaphiractic shock against xenogenic materials such as fetal bovine serum and trypsin derived from porcine intestinal mucosa. These xenogenic agents used for isolation and

culture of cells may contaminate with cells, and induced an exaggerated immune response to the host even with a small amount. Actually, the guideline of cell therapy specified by Japanese Ministry of Health notes that cautious monitoring of respiratory status and other vital signs should be performed during and after systemically injection of MSCs in human patients. Therefore, to assess an allergic risk after intravenous administration of BM-PACs in dogs is also required to ensure its safety.

On the other hand, in order to evaluate the efficacy of intravenous administration of BM-PACs in canine patients with subacute SCI, a novel non-invasive evaluation method should be developed. To confirm whether intravenously administrated BM-PACs home to injured spinal cord is a good indicator to predict the effect of cell-based therapy. The cell tracking method using fluorescent dye and IVIS which I used in the study in Chapter 3 cannot be applied in clinical cases, super paramagnetic iron oxide (SPIO) nanoparticle is available recently as an alternative tool for cell tracking. SPIO is applied to *in vivo* cell tracking using magnetic resonance imaging (MRI) in the recent studies on stem cell therapy for brain and spinal cord injury (Sykova *et al.*, 2007). SPIO is already used as contrast agents for MRI and provide the intent signal contrast changes, in particular on T2 and T2* weighted images (Mendonca Dias *et al.*, 1986).

Autologous MSCs transplantation are more desirable than allogenic MSCs transplantation because they show higher functional recovery, and lower immunological responses than those of allogenic MSCs (Jung *et al.*, 2009). However, it is difficult to apply autologous MSCs transplantation to SCI dogs in clinical medicine because of its preparation period and transplantation timing. While BM-PACs can proliferate rapidly enough to harvest adequate number of cells for clinical use in a shorter period comparing to conventional canine MSCs cultured by adhering culture of mononuclear cells in bone marrow. Therefore, using BM-PACs allows to expand the chances for autologous administration of canine MSCs in subacute phase of SCI even after a few days passed from the onset. For these reasons, using autologous BM-PACs is expected to be more appliable than conventional MSCs to SCI patients.

The objective of the study in this chapter is to assess the safety of intravenous administration of autologous BM-PACs and evaluate whether homing ability of BM-PACs to the injured tissue can be confirmed in healthy dog by detecting SPIO-labelled cells using MRI. Here, due to the ethical concerns, a canine skin injury model was used as an alternative to a SCI model because the expression of CXCL12 upregulation at the injury site in subacute phase of injury (Hu *et al.*, 2013) was observed as well as SCI.

Materials and Methods

Animals

Three healthy young beagle dogs (2 males and 1 female, 1 year-old, weighing an average of 11 kg) were employed to obtain bone marrow and skin injury. All animal experiments were approved by the Animal Care Committee of the Graduate School of Agricultural and Life Sciences, at the University of Tokyo (P18-133).

Culture of BM-PACs

Under general anesthesia, bone marrow samples were harvested and BM-PACs were cultured and cryopreserved as described in Chapter 1. Cryopreserved cells were thawed and cultured until cells reached over 80% confluency before use.

Skin injury model

After bone marrow aspiration, the lower back of the dog was shaved and disinfected, and a full thickness skin of 1 cm square was incised and removed. All dogs were administrated 2 mg/kg of robenacoxib (Onsior®, Elanco Animal Health, Greenfield, USA) and 20 μg/kg of buprenorphine for pain control.

Labelling and administration of BM-PACs

BM-PACs reached over 80% confluency were labeled with SPIO (Resovist®: Bayer HealthCare, Berlin, Germany) by incubating with 1 μg/ml of SPIO for 24 hr, according to a previous study (Zhang et al, 2009). Then the cells were detached and fluorescent-labeled with vivo track 680 as described in chapter 3. Intravenous administration of autologous BM-PACs were performed 10 days after the creation of skin injury according to the previous report which demonstrated significant upregulation of CXCL12 was observed after 1-2 weeks after skin injury in mice (Hu et al, 2013). To evaluate the influence of cell dose, low (1.25×10^7 cells/body), middle (2.5×10^7 cells/body) and high number (5.0×10^7 cells/body) of BM-PACs suspended in 50 ml of lactated Ringer's solution was administrated to each dog from chephalic vein through an infusion catheter over 30 min.

Safety assessment

To assess adverse reactions after autologous BM-PACs administration, heart rate, body temperature, and respiratory rate was monitored before and 1 hr, 1 day, and 7 days after administration. Complete blood count (CBC) and blood biochemistry were also examined from the blood samples taken before and after 1 hr and 7 days. Blood

biochemistry included total protein (TP), albumin (ALB), alkaline phosphatase (ALP) glutamic-pyruvic transaminase (GPT), blood urea nitrogen (BUN), creatinine (CRE), sodium (Na), potassium (K), chlorine (Cl), canine C-reactive protein (cCRP). To examine adverse events associated with possible pulmonary embolism, thoracic computed tomography (CT) was performed under general anesthesia before and 7 days after cell administration. CT scan was performed with clinical CT scanner (Aquilion prime, Canon, Tokyo japan). Routine examinations consisted of sequential 4-mm-thick sections obtained at 1-cm intervals (5 seconds, 120 kV).

MR imaging

Following CT scanning, MR imaging were performed using a 3.0T MR scanner (Vantage Galan 3T, Canon, Tokyo Japan) to detect the magnetic-labeled cells. T2-weighted images (repetition time: 3,000 ms, echo time: 45 ms, FOV: 125.6, slice thickness: 1 mm) were acquired from sagittal slices including injured area.

Histological analysis of injured skin

To histologically confirm whether BM-PACs homed to injured skin, injured skin samples were collected after MR scanning. Collected tissues were placed in 4% PFA

and immediately subjected to visualization of fluorescent-labeled cells using IVIS. Then, samples were kept in 4% PFA for overnight and dehydrated by 20 % and 30 % sucrose. After frozen-embedded with OCT compound (Tissue-TeK® O.C.T compound, Sakura Fine-tek), serial transverse sections of injured skin were obtained at 4-μm thickness using a cryotome (Laica, Deerfield, IL). Prussian blue method was used to detect iron within transplanted cells. Sections were washed in phosphate-buffered saline (PBS) (without Ca^2 and Mg) to remove the excess of contrast agent. Prussian blue (PB) staining was performed by incubation in a 1:1 mixture of 1% HCl (Fujifilim Wako) and 2% potassium ferrocyanide (Muto pure chemicals, Tokyo, Japan) for 30 minutes at room temperature (24°C). After washed in DW, sections were counter stained with nuclear fast red (Muto pure chemicals).

Results

Safety of intravenous administration of BM-PACs

There were no noticeable changes in vital signs in the dogs administrate the different number of BM-PACs (Fig. 1). CBC and blood chemistry profiles of all dogs were maintained within normal ranges before and after cell administration (Fig. 2, Fig. 3).

Thoracic CT scan obtained before and 7 days after BM-PACs administration revealed no adverse event suggesting pulmonary embolism and infarction even in the dog administrated high number of BM-PACs (Fig. 4).

Detection of homing cells using MR scanning and IVIS

T2 weighted MR imaging revealed that there were no apparent hypointensity signals indicating the presence of SPIO-labeled BM-PACs in the injured skin area (Fig. 5). On the other hand, fluorescent signals were detected in the central area of the skin lesion of the dogs administrated the low and high number of BM-PACs (Fig. 6). The signal intensity detected was supposed to be relative to the number of cells administrated. However, no apparent fluorescent signal was detected in the lesion of the dog administrated the middle dose of BM-PACs.

Histopathological findings in injured skin after intravenous administration of BM-PACs

Histological examination revealed that Prussian blue-positive cells with fibroblastic morphology resided in the lesion in which fluorescent signal was also detected. The numbers of cells observed was likely to be relative to the signal intensity detected by IVIS. On the other hand, there was few cells positive for Prussian blue in the injured skin of the dog administrated the middle doze of BM-PACs (Fig. 6, Fig. 7)

Discussion

In this chapter, I investigated the safety of intravenous administration of autologous BM-PACs with different number of BM-PACs ranging 1.25-5.0 × 10^7 cells per body. No adverse event was observed by monitoring vital sings even in the dog administrated larger number of BM-PACs. Hematological and blood chemical parameters showed no obvious change after cell administration. Normal WBC counts and blood CRP level denied the occurrence of severe inflammation following to an anaphylactic or allergic response. Thoracic CT scanning also showed no apparent evidence of pulmonary embolism and inflammatory sings in the lung. Therefore, it is expected that intravenous administration of autologous BM-PACs within the range of number used in this study has adequate safety for clinical application. Kim et al. reported intravenous administration of 1×10^7 canine adipose tissue-derived MSCs to dogs experimentally induced SCI showed therapeutic effects on functional recovery. Therefore, the number of BM-PACs used in this study is expected to contribute functional recovery as well as safety.

Fluorescent signals were detected using IVIS in the injured skin of the dog administrated small and large number of BM-PACs. Although the reason that fluorescent signal was not detected in the injured skin of the dog administrated middle

dose of BM-PACs was unclear, it was suggested that intravenously administrated autologous BM-PACs had potential to home to the injured tissue.

In accordance with this result, Prussian blue positive cells were also found in the injured skins where the fluorescent signals were detected. The number of Prussian blue positive cells were relative to the fluorescent signal intensity, thus the number of cells homed to the injured skin could be estimated by the fluorescent signal intensity. Concerning the fact that there were also few cells positive for Prussian blue in the injured skin of middle dose administrated dog, it was suggested that the homing cell number might be too small to be detected in IVIS. I also investigated the homing of autologous BM-PACs to the injured site by tracking magnetic labeled cells using MRI. However, no obvious signals were observed in any injured skins. Even though a number of Prussian blue positive cells were observed in the skin of the dog administrated high dose of BM-PACs, MR scanning failed to detect the magnetic signal. According to a clinical trial in human amyotrophic lateral sclerosis patients, 2.5×10^6 human MSCs labeled with SPIO homed into the damaged spinal cord and were successfully detected as the hypointense signals in T2 weighted sequence using 1.5T MRI (Karussis *et al.*, 2010). It was also suggested that a greater number of cells homed into the injured area and a larger amount of SPIO uptaken into each cell enhanced the detectability of

magnetic signal (Lamanna *et al.*, 2017; Kraitchman *et al.*, 2003; Frank *et al.*, 2003). The number of BM-PACs administrated to the dogs (1.25-5.0$\times 10^7$ cells) in this chapter was considered to be adequate, however, it was likely that the homing cell number was too small to be detectable. So far, to improve in-take efficiency of SPIO, there have been explored various agents such as poly-L-lysine and dextran. Combined use of these agents may be useful to enhance the magnetic signals of BM-PACs.

In conclusion, the study in this chapter may guarantee the safety of intravenous administration of autologous BM-PACs. Although further investigation to develop *in vivo* cell tracking method using MR scanning should be performed, intravenous administration of autologous BM-PACs can be applied to dogs with subacute SCI with evidence-based efficacy and safety.

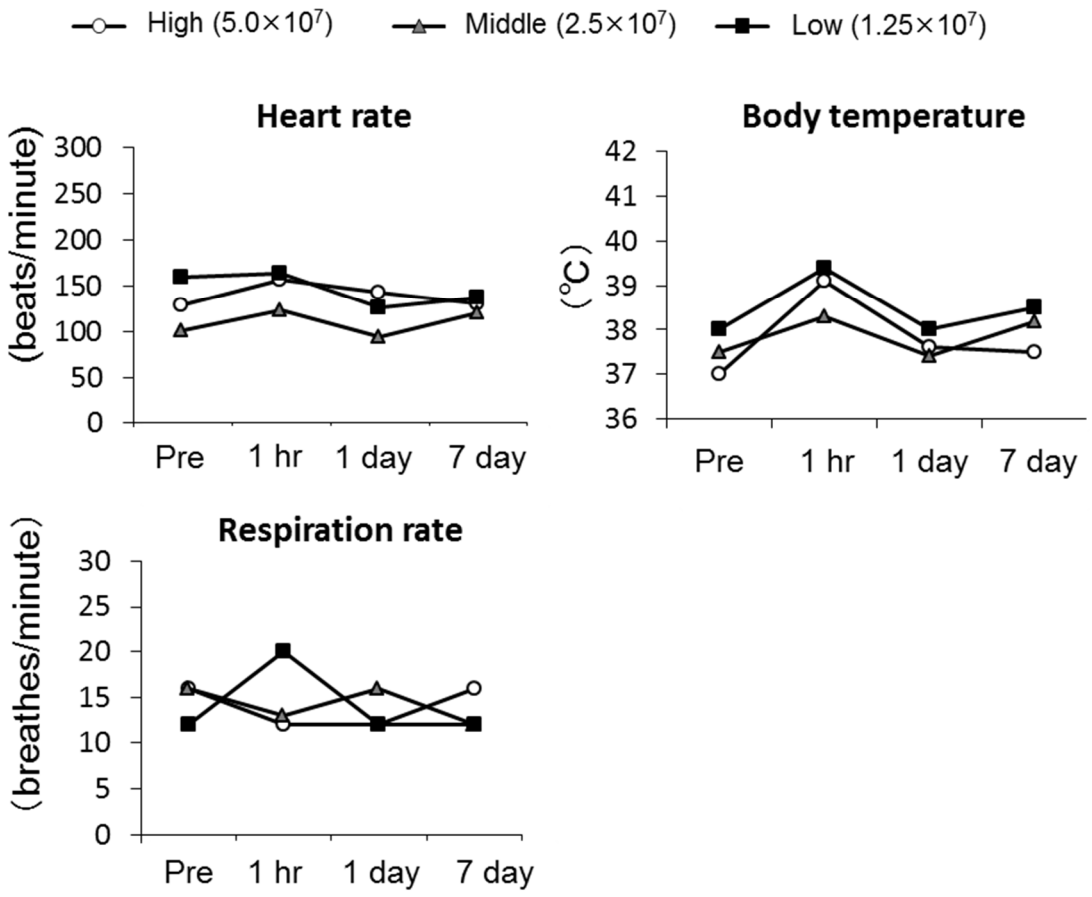

Fig.1　Vital sings before and after intravenous administration of autologous BM-PACs

There were no noticeable changes in vital signs in all dogs administrated the different number of BM-PACs.

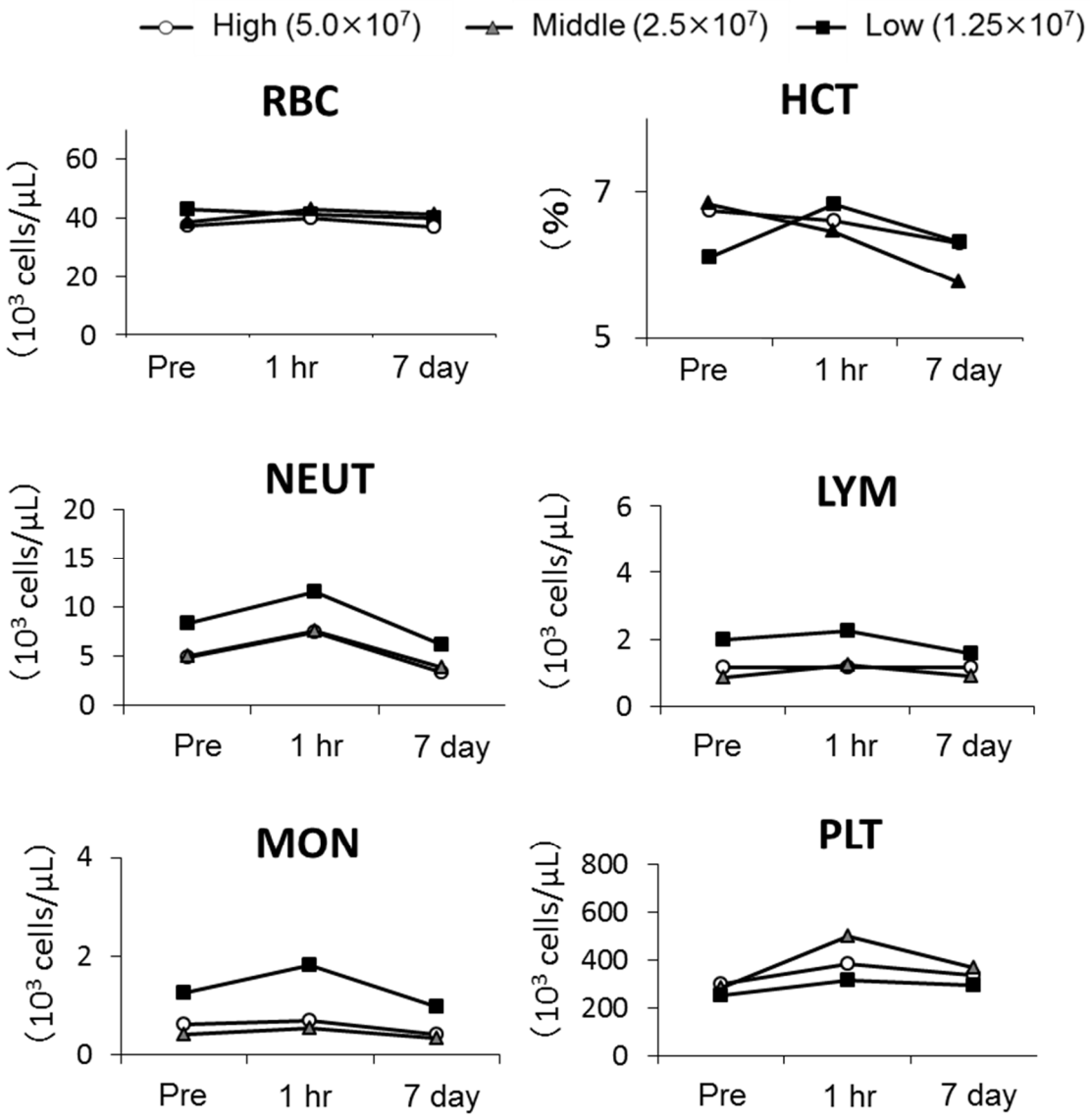

Fig.2　Complete blood count after intravenous BM-PACs administration

Analysis were performed a total of three times, before and 1h, 7day after cell administration. All groups were in normal ranges. RBC; red blood cell, HCT; hematocrit, NEUT; neutrophil, LYM; lymphocyte, MON; monocyte, PLT; platelet.

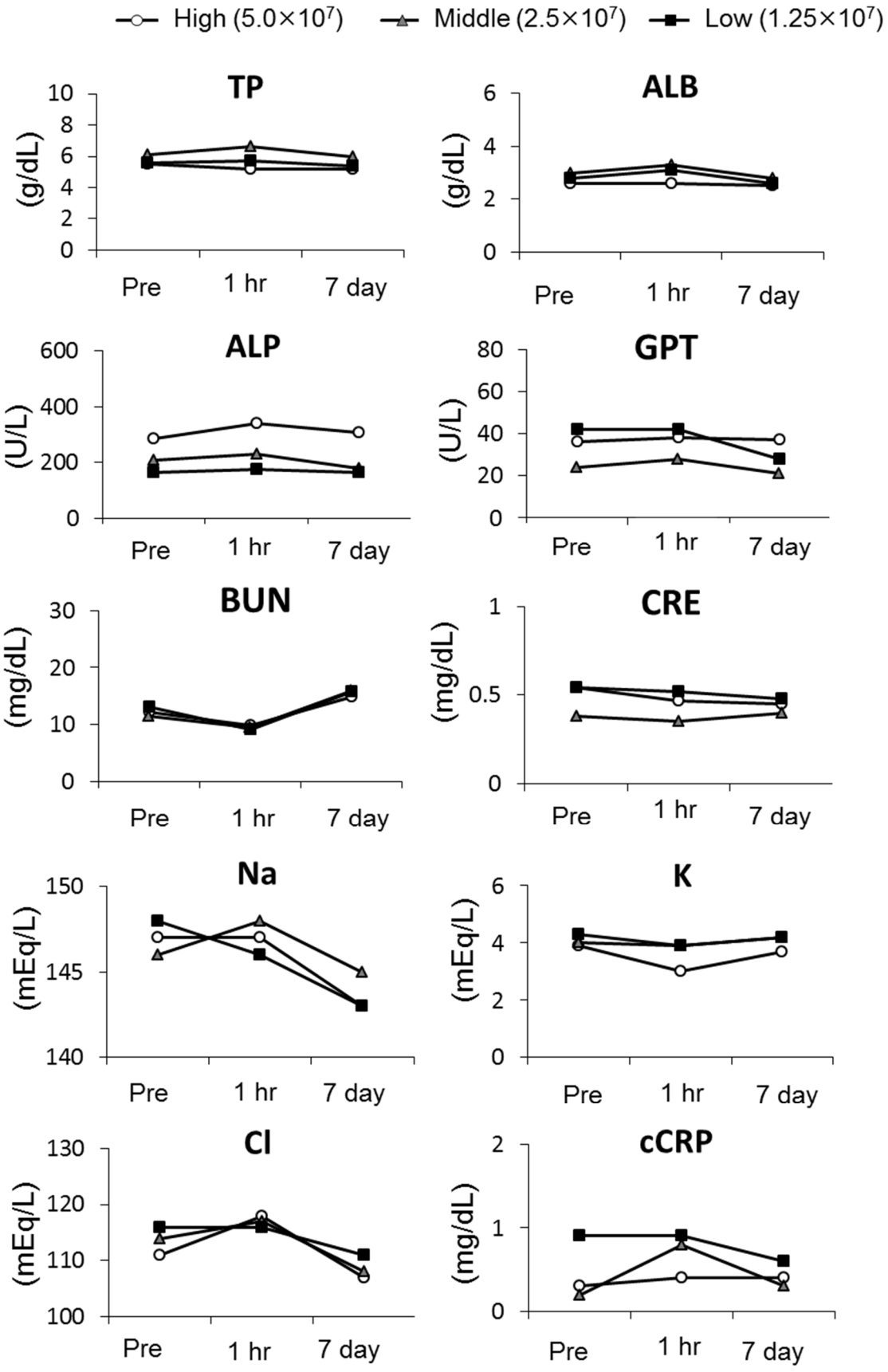
High (5.0×10^7)
Middle (2.5×10^7)
Low (1.25×10^7)
TP
(g/dL)
ALB
(g/dL)
ALP
(U/L)
GPT
(U/L)
BUN
(mg/dL)
CRE
(mg/dL)
Na
(mEq/L)
K
(mEq/L)
Cl
(mEq/L)
cCRP
(mg/dL)
Pre
1 hr
7 day

Fig.3　Blood chemistry before and after intravenous BM-PACs administration
No noticeable changes were observed in the results of biochemistry. All examination items are within normal ranges before and after cell administration. TP; total protein, ALB; albumin, ALP; alkaline phosphatase; GPT; glutamic-pyruvic transaminase, BUN; blood urea nitrogen, CRE; creatinine, Na; sodium, K; potassium, Cl; chlorine, CRP; C-reactive protein.